Nanostructured Thin Film Thermoelectric Composite Materials Using Conductive Polymer PEDOT:PSS

by

Chris A. Kuryak

B.S. Mechanical Engineering

University of Texas at Austin, 2006
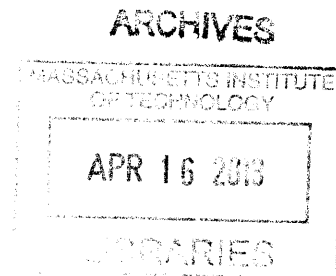
SUBMITTED TO THE DEPARTMENT OF MECHANICAL ENGINEERING

IN PARTIAL FULFILLMENT OF THE REQUIREMENTS FOR THE DEGREE OF

MASTER OF SCIENCE IN MECHANICAL ENGINEERING

AT THE

MASSACHUSETTS INSTITUTE OF TECHNOLOGY

February 2013

© 2013 Massachusetts Institute of Technology.

Signature of Author...

Department of Mechanical Engineering

November 7, 2012

Certified by...

Yang Shao-Horn

Gail E. Kendall Associate Professor of Mechanical Engineering

Thesis Supervisor

Accepted by...

David E. Hardt

Ralph E. and Eloise F. Cross Professor of Mechanical Engineering

Chairman, Department Graduate Committee

Nanostructured Thin Film Thermoelectric Composite Materials
Using Conductive Polymer PEDOT:PSS
By

Chris A. Kuryak

Submitted to the Department of Mechanical Engineering
on November 7, 2012 in Partial Fulfillment of the
Requirements for the Degree of Master of Science in
Mechanical Engineering

ABSTRACT

Thermoelectric materials have the ability to convert heat directly into electricity. This clean energy technology has advantages over other renewable technologies in that it requires no sunlight, has no moving parts, and is easily scalable. With the majority of the unused energy in the United States being wasted in the form of heat and the recent mandates to reduce greenhouse gas emissions, thermoelectric devices could play an important role in our energy future by recovering this wasted heat and increasing the efficiency of energy production. However, low conversion efficiencies and the high cost of crystalline thermoelectric materials have restricted their implementation into modern society. To combat these issues, composite materials that use conductive polymers have been under investigation due to their low cost, manufacturability, and malleability. These new composite materials could lead to cheaper thermoelectric devices and even introduce the technology to new application areas. Unfortunately, polymer composites have been plagued by low operating efficiencies due to their low Seebeck coefficient.

In this research, we show an enhanced Seebeck coefficient at the interface of poly(3,4-ethylenedioxythiophene) poly(styrenesulfonate) (PEDOT:PSS) spin coated onto silicon substrates. The maximum Seebeck coefficient achieved was 473 uV/K with a PEDOT:PSS thickness of 7.75 nm. Furthermore, the power factor of this interface was optimized with a 15.25 nm PEDOT:PSS thickness to a value of 1.24 uV/K^2-cm, which is an order of magnitude larger than PEDOT:PSS itself. The effect of PEDOT:PSS thickness and silicon thickness on the thermoelectric properties is also discussed.

Continuing research into this area will attempt to enhance the power factor even further by investigating better sample preparation techniques that avoid silicon surface oxidation, as well as creating a flexible composite material of PEDOT:PSS with silicon nanowires.

Thesis Supervisor: Yang Shao-Horn
Title: Gail E. Kendall Associate Professor of Mechanical Engineering

Acknowledgements

I am very thankful to my advisor, Professor Yang Shao-Horn, for taking the chance to let me investigate a subject that I was interested in, but which I knew nothing about. Her guidance and support have led to the significant discoveries in this work, and her questions have given me a more fundamental approach to my scientific endeavors.

I am lucky to have such a smart, supportive, and kind post-doc advisor as Chris Carlton. I can't count how many times I have come to him with ideas, questions, and failures, but he always showed genuine interest to help me solve the problems.

Without the help from my fellow workers in the electrochemical energy lab (EEL), I would have never finished this work. Everyone that worked in the lab in 2011 and 2012 has in some way participated and helped me with this research. I had heard stories that some graduate labs were competitive and unfriendly, but the EEL has been the complete opposite. Everyone has always been helpful, knowledgeable, and easy to get along with. I am sincerely grateful to have worked among such an incredible group of people. A special thanks to: Seung Woo Lee for the overall guidance and experimental advice, Joe Elias for being my lab advisor and answering my endless number of questions, and Tian Ming for his help with sample preparation and willingness to teach me solid state physics.

I would like to thank Shuo Chen for her collaboration during the beginning of this research and helping me get started with my experiments. I would also like to thank Keivan Esfarjani for his genuine interest in my project and help with answering all of my physics questions, as well as Yongjie Hu for his help with the silicon sample preparation. Additionally, I'd like to thank Professor Gang Chen for the challenging and fruitful discussions on interface physics and help in creating the future experiments and direction of this project.

My family has always been my biggest supporter and to them I am eternally in debt. I definitely would not have made it to this point without them and their support through this research has been profound. It's easy to lose your perspective on life and research while at MIT, and they have always kept me grounded.

Table of Contents

List of Figures

coefficient shows only a small decrease with the addition of DMSO. The error bars are one standard deviation from the mean.

List of Tables

1 Introduction

1.1 Motivation and Challenges

As energy demand around the world increases and the amount of non-renewable fossil fuels decreases, the need for sustainable renewable energy sources is evident. In addition to the growing demand for energy, there is also a push for reducing the amount of emitted pollution, in the form of greenhouse gasses, by using clean energy sources. In the United States, the official goal is to reduce greenhouse gas emissions 17% below 2005 levels by the year 2020.[1] A solution to both of these energy problems can be realized by reducing the amount of wasted energy. The United States wastes about 58% of the energy it produces, the majority of which takes the form of waste heat (Figure 1). Thermoelectric materials, which directly convert heat to electricity, have the ability to transform this wasted heat into useful energy. Therefore, thermoelectric technology has the potential to increase the efficiency of energy production and reduce the amount of pollution emitted.
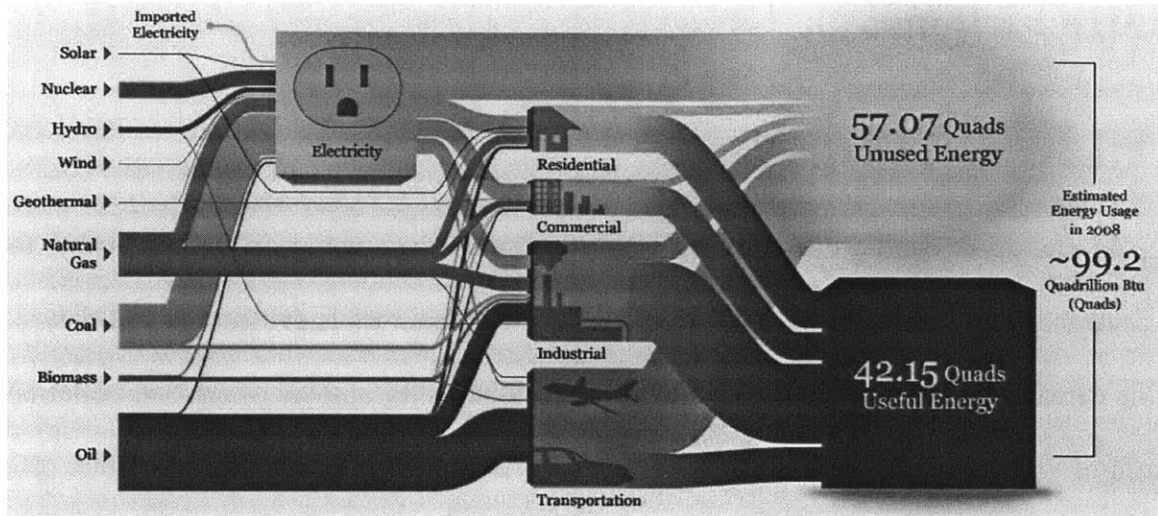
Figure 1: The energy flow of the United States from 2008. Sources of energy are on the left and uses of the energy on the right. About 58% of the energy goes unused. The majority of this unused energy is in the form of waste heat.[2]

Furthermore, thermoelectric technology is not limited to converting heat into energy but can also be used in the reverse situation as a device to provide active heating or cooling. This makes thermoelectric materials a marketable and versatile technology. Current applications for this technology include consumer refrigeration, consumer heating, and power generation for space exploration. But the low energy conversion efficiency of this technology often makes it not a cost-effective solution and has limited its use in modern society. This has caused much of the research over the past several decades to be focused on increasing the efficiency of thermoelectric materials.[3] With increased conversion efficiency, potential applications include car exhaust and power plant waste heat recovery, electronic device cooling, and body heat power generation. The majority of thermoelectric research to date has been focused on crystalline semiconductor materials. Recently, however, the investigation of polymer-composite materials has become of interest due to their low cost, manufacturability, and favorable thermoelectric properties[4-6]. The work of this thesis focuses on increasing the thermoelectric efficiency of

conductive polymer poly(3,4-ethylenedioxythiophene) poly(styrenesulfonate) (PEDOT:PSS) via nanostructuring with undoped silicon. First, we introduce the background and mechanics of thermoelectric energy conversion. Then we explain our sample creation process and thermoelectric property measurement devices. Next, we benchmark our preliminary data against existing literature data. Lastly, we show the properties of nanoscale thin films of PEDOT:PSS and how the properties change when the films interact with an undoped silicon substrate.

1.2 Thermoelectric Operation Overview

Thermoelectric materials have two forms of operation: power generation and refrigeration. In a power generation setup, the thermoelectric material is supplied with a temperature gradient to create electricity (Figure 2a). In a refrigeration setup, the thermoelectric material is supplied with electricity to create a temperature gradient (Figure 2b).
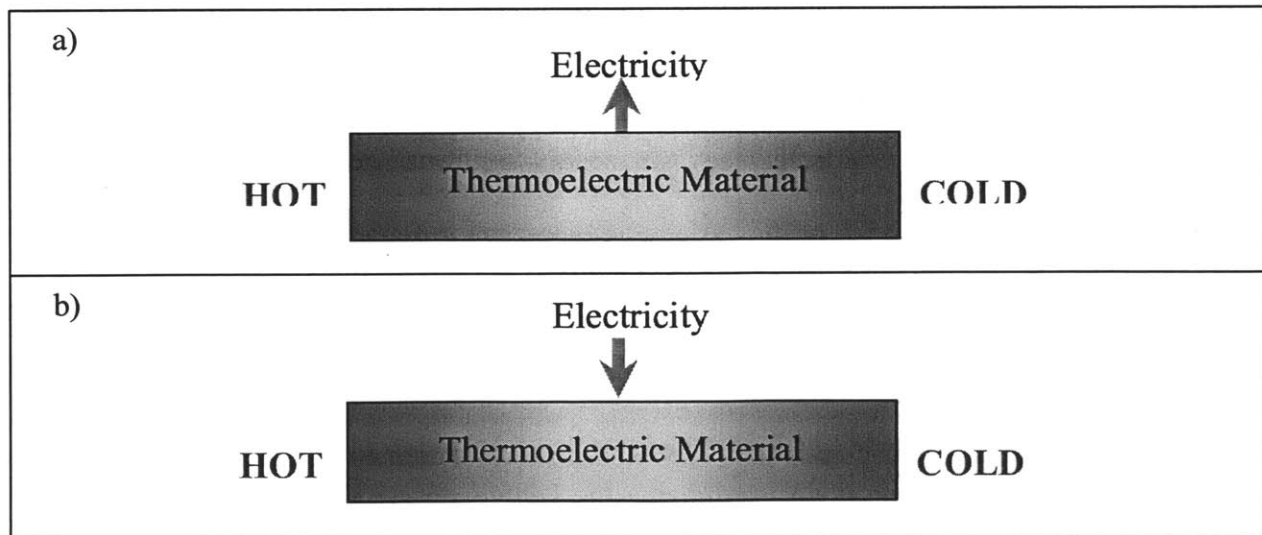
Figure 2: Basic operation of a thermoelectric device in a) power generation setup and b) refrigeration setup.

For the remainder of this work, we will focus on explaining thermoelectric materials through the power generation configuration. The voltage that can be generated by a thermoelectric material is governed by its Seebeck coefficient (see section 1.2.4). Though the Seebeck coefficient is a key property in determining how effective a thermoelectric material converts heat into electricity, the overall efficiency of a device involves many more components.

1.2.1 Device Efficiency and the Thermoelectric Figure of Merit

The thermoelectric device efficiency (η) is a product of two different constituents: Carnot efficiency and material efficiency (Eq. 2).[7] The Carnot efficiency is a thermal efficiency that is limited by the second law of thermodynamics using the hot side (T_h) and the cold side (T_c) temperatures. The material efficiency is governed by the properties of the thermoelectric material used in the device.

$$\eta = \underbrace{\left(1 - \frac{T_c}{T_h}\right)}_{\textbf{Carnot}} \underbrace{\frac{\sqrt{1 + ZT_M} - 1}{\sqrt{1 + ZT_M} + \frac{T_c}{T_h}}}_{\textbf{Material}}$$

(Eq. 2)

The material efficiency contains a variable known as the dimensionless figure of merit (ZT). This variable is derived from maximizing the Peltier refrigeration efficiency for a given thermoelectric material.[8] One can determine the dimensionless figure of merit using the electrical conductivity (σ), Seebeck coefficient (S), thermal conductivity (κ), and mean temperature (T_m)

16

of the material (Eq. 3).[8] The mean temperature is defined as the average temperature between the

hot and cold sides ($T_m = [T_h+T_c]/2$).

$$ZT = \frac{S^2 \sigma T_M}{\kappa}$$

To maximize the efficiency (Eq. 2) of a thermoelectric device, one needs to maximize the

dimensionless figure of merit (ZT). Therefore, when investigating thermoelectric materials, the

primary goal, and indeed the focus of this thesis, is to increase the thermoelectric figure of merit

(ZT) of the material.

1.2.2 Thermal Conductivity (κ)

The total thermal conductivity (κ) of a material quantifies how well it conducts heat.

Materials that conduct heat well, such as copper, have a high thermal conductivity. Materials that

conduct heat poorly, such as polymers, have a low thermal conductivity. The total thermal

conductivity is composed of two parts: the lattice thermal conductivity (κ_l) and the electronic

thermal conductivity (κ_e) (Eq. 4). The lattice component (κ_l) comes from lattice vibrations that

are transmitted through the material. These lattice vibrations are also known as phonons. The

electronic component of thermal conductivity comes from the ballistic transport of electrons as

they move through the material (κ_e).

$$k = k_e + k_l$$

It can be seen that in order to maximize ZT (Eq. 3), we want to minimize the thermal conductivity (κ).

1.2.3 Electrical Conductivity (σ)

The electrical conductivity (σ) of a material quantifies how well it conducts electrons. Materials that conduct electrons well, such as copper, have a high electrical conductivity; whereas, materials that conduct electrons poorly, such as wood, have a low electrical conductivity. The electrical conductivity (σ) of a material is a product of its carrier concentration (n), mobility (μ), and the elementary charge constant (e) (Eq. 5). The carrier concentration (n) is the concentration of electrons in the valence band or holes in the conducting band of a material. The mobility (μ) describes how easily the carriers can move through the material. The elementary charge constant (e) is defined as the electric charge carried by a single electron (1.6e-19 C).

$$\sigma = ne\mu$$

(Eq. 5)

In order to maximize ZT (Eq. 3), we want to maximize the electrical conductivity (σ).

1.2.4 Seebeck Coefficient (S)

The Seebeck coefficient of a material quantifies the amount of voltage generated (ΔV) across a given temperature gradient (ΔT). Semiconducting materials can have excess charge

18

carriers (holes or electrons) in their electronic structure (Figure 3a). If excess holes are present, then the semiconductor is considered p-type. If excess electrons are present, the semiconductor is considered n-type. When a temperature gradient is created across the material, the excess charge carriers will migrate to the cold side of the material (Figure 3b). The "build-up" of carriers on the cold side creates a voltage potential across the material. When the material is then connected across an external load, a current will flow creating a power output (Figure 3c).
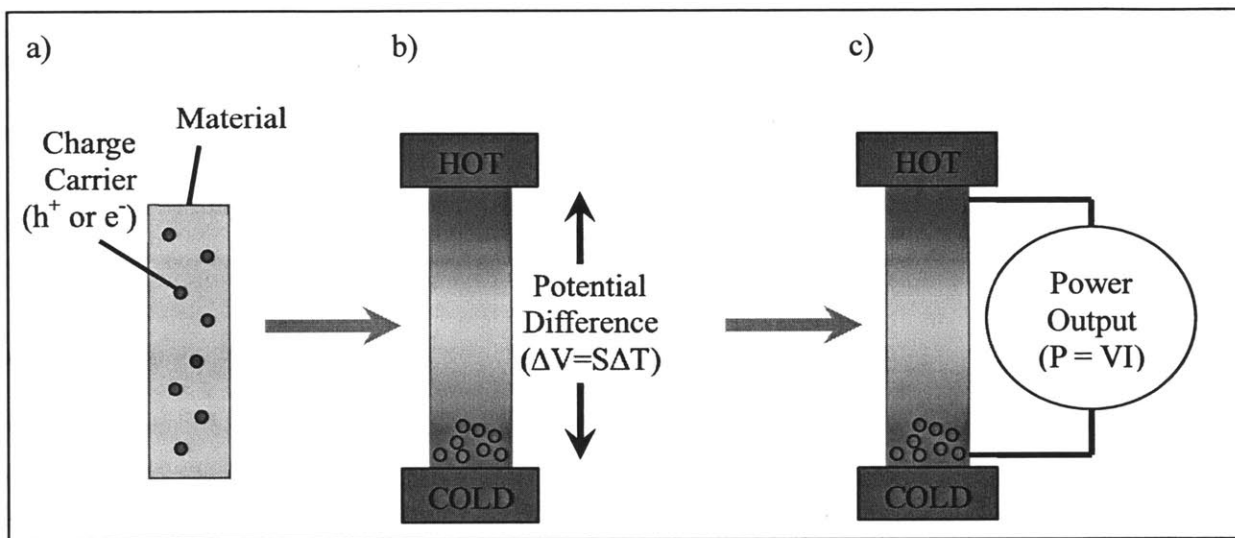
Figure 3: Description of Seebeck coefficient in a semiconducting material. a) The semiconductor has excess charge carriers. b) In the presence of a temperature gradient, these carriers will "build-up" on the cold side of the material creating a voltage potential across the material. c) Completing the circuit across an external load will induce a current and create power.

The ratio of voltage generated (ΔV) to temperature gradient (ΔT) is defined as the Seebeck coefficient (S) (Eq. 6). It is also worth noting that the Seebeck coefficient is inversely proportional to the carrier concentration (n) (Eq. 7). This is contrary to the electrical conductivity, which varies directly with the carrier concentration (n) (Eq. 5).

$$S = -\frac{\Delta V}{\Delta T}$$

<div align="right">(Eq. 6)</div>

$$S \propto \frac{1}{n}$$

<div align="right">(Eq. 7)</div>

In order to maximize ZT (Eq. 3), we want to maximize the Seebeck coefficient (S).

1.3 Current Thermoelectric Materials vs. Polymer Materials

Current thermoelectric material research focuses on nanostructured crystalline semiconductor materials.[3,9] These semiconductors are usually heavily doped to achieve the best dimensionless thermoelectric figure of merit (ZT). Commercially available state-of-the-art thermoelectric materials are typically based on Bi_2Te_3 and Sb_2Te_3 –based alloys and have a room temperature dimensionless figure of merit (ZT) near 1.[9,10] The disadvantages of using these crystalline semiconductor materials are that they are expensive, rigid, and sometimes toxic. Polymers, on the other hand, are less expensive, malleable, non-toxic materials with a high degree of manufacturability. These polymeric advantages could open new areas for thermoelectric applications and make the technology a more cost-effective energy solution. However, compared to crystalline semiconductor materials, polymers have a much lower dimensionless thermoelectric figure of merit (ZT) that must be improved in order to become competitive.

The thermoelectric properties of a typical Bi_2Te_3-based alloy at room temperature can be found in Table 1. The dimensionless figure of merit of this semiconductor is more than an order

of magnitude larger than that of the conductive polymer PEDOT:PSS. When comparing the individual properties of each material, it can be seen that the polymer can achieve a similar electrical conductivity and a more favorable thermal conductivity. However, the Seebeck coefficient of the conductive polymer is an order of magnitude less than the Seebeck coefficient of the crystalline semiconductor. From this evidence it can be seen that in order to make conductive polymers more competitive with crystalline semiconductors for use as thermoelectric materials, the Seebeck coefficient must be enhanced greatly. To this end, it was the goal of this research to enhance the Seebeck coefficient of conductive polymer PEDOT:PSS by investigating its interface interaction with undoped silicon, a high-Seebeck material.

BiSbTe bulk alloy		**PEDOT:PSS**
1200	σ [S/cm]	945
190	S [μV/K]	22.2
1.1	κ [W/mK]	0.17
1.2	ZT	0.08

Table 1: Thermoelectric properties of a crystalline semiconductor and conductive polymer. The semiconductor is a bulk nanocrystalline alloy of BiSbTe.[11] The conductive polymer is DMSO-treated poly(3,4-ethylenedioxythiophene) poly(styrenesulfonate).[4] In order to compare favorably with the ZT of crystalline semiconductors, the Seebeck of conductive polymers must be increased.

1.4 Previous Work

The path to this research was inspired by results from previous publications. These publications included three main discoveries:

1) The thermoelectric properties of conductive polymer composites when combined with other materials did not follow the particle mixture rule.[12]

2) The electrical conductivity of polymer PEDOT:PSS was greatly enhanced with the addition of solvent dimethyl sulfoxide (DMSO).[4]

3) The Seebeck coefficient of conductive polymer composites was increased when combined with high Seebeck coefficient materials.[5]

The results from these publications helped form the foundation onto which our research is built.

In 2010, Yao et al. published results showing that conductive polymer composite materials do not follow the particle mixture rule when combined with other materials.[12] This was an important discovery because it provided a basis for combining unlike materials in an effort to enhance the thermoelectric properties of the composite. In the experiment, polyaniline, a polymer with low thermal conductivity, was combined with varying amounts of single-walled carbon nanotubes (SWNT), which has a high electrical conductivity. The composite material had both the enhanced electrical conductivity of the carbon nanotubes and the low thermal conductivity of the polyaniline (Figure 4).
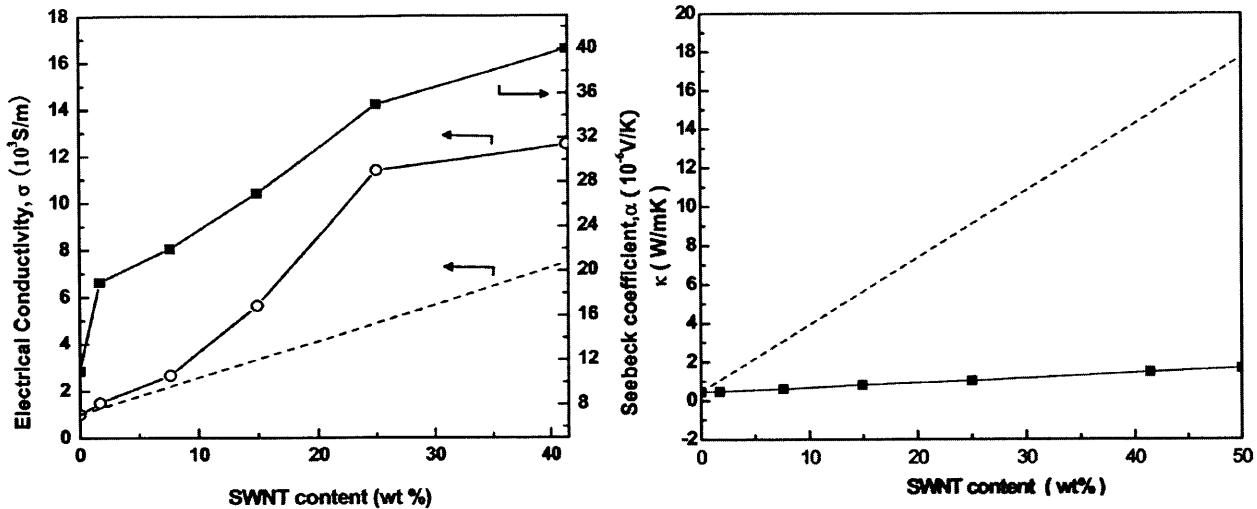
Figure 4: Thermoelectric properties of a polyaniline/SWNT composite material. The composite had both the enhanced electrical conductivity of SWNTs and the low thermal conductivity of polyaniline. Also, the properties of the composite did not follow the particle mixture rule (dotted lines).[12]

The results from Yao et al. also showed that the composite material did not follow the particle mixture rule (dotted lines in Figure 4). In particular, with regard to the thermal conductivity (κ), the composite maintains a low value (~1.5 W/mK) even at 50 wt.% SWNT. The ability for polymer-composite materials to combine the favorable thermoelectric properties of its constituents, in this case high electrical conductivity and low thermal conductivity, provided proof that mixing materials could be a way to create enhanced thermoelectric materials.

Contrary to the research of Yao et al., we did not want to use carbon nanotubes as a way to increase the electrical conductivity of our composite. Rather, we wanted to use a polymer with innate high electrical conductivity and combine it with a high-Seebeck material. A suitable polymer with high electrical conductivity was PEDOT:PSS mixed with DMSO. Zhang et al. have shown that the electrical conductivity of Clevios PH1000 PEDOT:PSS can be increased almost three orders of magnitude when mixed with the solvent DMSO. Specifically, they achieved an electrical conductivity of 945 S/cm at 5 wt.% DMSO (Figure 5).[4] This increase in

electrical conductivity also resulted in only a small decrease in the Seebeck coefficient of the material.
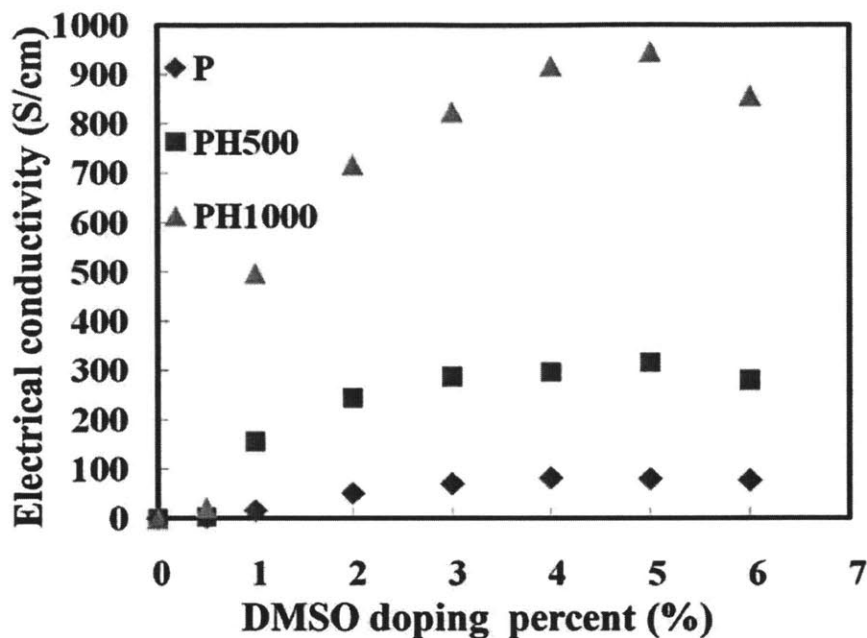
Figure 5: The electrical conductivity of PEDOT:PSS with increasing DMSO doping percent. The electrical conductivity of Clevios PH1000 PEDOT:PSS reaches 945 S/cm at 5 wt.% DMSO doping.[4]

It was unclear why adding solvent to the PEDOT:PSS increased the electrical conductivity so dramatically. One argument was that the solvent created a conformational change that swells the polymer chains and possibly elongates the clusters to impose better connectivity.[13,14] Another argument provided supporting evidence that the solvent removes PSS from the sample, the insulating portion of the PEDOT:PSS polymer, which increased the PEDOT to PSS ratio.[15] Regardless of the cause for this increase, when we look back at Table 1, it can be seen that 945 S/cm was near the electrical conductivity achieved by modern day

thermoelectric materials. The results of Zhang et al. provided the basis for using Clevios PH1000 doped with DMSO solvent as the conductive polymer for our studies.

The research of See et al. in 2010 showed that mixing a conductive polymer with a high Seebeck material can have a favorable increase in the overall Seebeck coefficient of the composite material.[5] In this study, tellurium nanowires were passivated with conductive polymer PEDOT:PSS (PH1000). The resulting composite possessed a Seebeck coefficient of almost an order of magnitude greater than PEDOT:PSS alone (Table 2).

system	σ (S/cm)	S (μV/K)	$S^2\sigma_{max}$ (μW/(m K^2))	κ (W/(m K))	ZT_{max}
hybrid	19.3($\pm$2.3)	163($\pm$4)	70.9	0.22−0.30^a	0.10
PEDOT:PSS	1.32($\pm$0.12)	18.9($\pm$0.2)	0.05	0.24−0.29	6 $\times$ 10^{-5}
Te NWs	0.08($\pm$0.03)	408($\pm$69)	2.7	2^b	4 $\times$ 10^{-4}

Table 2: Thermoelectric properties of PEDOT:PSS, tellurium nanowires, and the nanowire-polymer composite. The Seebeck of the composite increases 8.6 times over the Seebeck of the PEDOT:PSS alone. The resulting ZT is near 0.1, only one order of magnitude below crystalline semiconductor thermoelectric materials.[5]

The composite, which was 85% tellurium by weight, obtained a dimensionless figure of merit (ZT) near 0.1. This ZT was only one order of magnitude smaller than the crystalline thermoelectric materials currently used today (Table 1). The results of See et al. proved that large increases in the Seebeck coefficient of polymer composite materials could be achieved when combined with high Seebeck materials. We also believed that a possible cause for this increase is due to the interaction of the PEDOT:PSS and tellurium nanowires at their interface. These results further supported our effort to investigate the thermoelectric properties at the interface of PEDOT:PSS and silicon to better understand the interaction that may be occurring.

2 Experimental

2.1 Measurement Devices

In order to calculate and compare the performance from any samples we created, the thermoelectric properties needed to be measured. As seen in Equation 3, these properties included the Seebeck coefficient (S), electrical conductivity (σ), the mean temperature (T_m), and the thermal conductivity (κ).

2.1.1 Thermal Conductivity (κ)

The thermal conductivity (κ) of polymers is inherently low, and PEDOT:PSS has values near 0.3 W/mK (Table 2).[5] It has also been shown that even with the addition of high thermal conductivity additives, the overall thermal conductivity of polymer composites remains low and does not follow the particle mixture rule (Figure 4).[12] In addition, the focus of this study is to increase the Seebeck coefficient of the polymer composite; therefore, the thermal conductivity was not measured because it was assumed to stay inherently low and not fluctuate greatly in our experimental samples.

2.1.2 Electrical Conductivity (σ)

The electrical conductivity (σ) of our samples was measured with a four-point probe device (LucasLabs Pro4-4400 with Keithley 2400 Source Meter and Pro4 Software v1.2.7). To explain how the system works, first we must explain how to measure electrical conductivity. Electrical conductivity (σ) is the reciprocal of electrical resistivity (ρ). Electrical resistivity is

defined as the resistance of the material (R) multiplied by the area through which electrons travel (A), divided by the length over which the electrons travel (l). The resistance (R) can be found through ohm's law by dividing the voltage (V) by the current (I). Assuming a rectangular cross-section, the area (A) can be further defined as the product of width (w) and thickness (t) (Eq. 8,9).

$$\rho = \frac{V/l}{I/(wt)}$$ (Eq. 8)

$$\sigma = \frac{1}{\rho}$$ (Eq. 9)

The circuit for measuring electrical conductivity via a 4-point method is shown in Figure 6. Though two contact points is all that is required for providing current and measuring voltage of a material, the four-point method eliminates any contact resistance in the voltage measurement. The device used for these experiments provided a current (I) and measured the voltage drop (V) in the sample. The length (l) was simply the spacing of the probe tips, and the width (w) was estimated by the LucasLabs software. The thickness (t) of each sample was measured via surface profilometry and entered into the software.
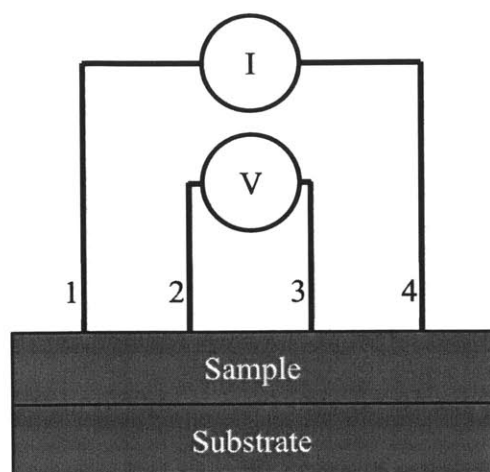
Figure 6: Four-point electrical conductivity circuit. Current is supplied between pin 1 to pin 4. Voltage is measured between pin 2 to pin 3.

The probe head setup used in these experiments had four osmium pins with a spacing of 1.02 mm. The spring force of the pins was 0.44 mN (45 mg specification) and the radius of the pins was either 0.04 mm or 0.254 mm. When deciding between which pin radius to use, it was found that both radii produced the same results for the PEDOT:PSS samples on glass substrates. However, for the spin coated PEDOT:PSS samples on glass substrates, the larger 0.254 mm radius pins made better connection with the sample and had more consistent results. It was believed that the inconsistencies encountered while using the small pins were a result of the soft polymer being penetrated and pushed away by the smaller radius pins, causing a poor electrical connection between the device and polymer. Therefore, the larger radius (0.254 mm) pins were used for all electrical conductivity measurements of spin coated samples on glass substrates. For the spin coated samples on silicon substrates, the small radius pins were used in all electrical conductivity measurements because we wanted to measure the properties at the interface of the two materials, and penetrating the PEDOT:PSS layer with the small radius tips helped achieve

this goal. For all electrical conductivity measurements of all samples, the NIST standard dual-configuration mode was used.[16]

The thickness (t) of each sample was measured with surface profilometry using a KLA Tencor P-16+. To obtain an estimate of the thickness, three lines were scratched onto the sample using a plastic knife thereby exposing the substrate underneath. A plastic knife was used to make the scratches, as opposed to a razor blade, to ensure that the substrate was not also scratched. The step height was measured at each of these scratches (Figure 7).
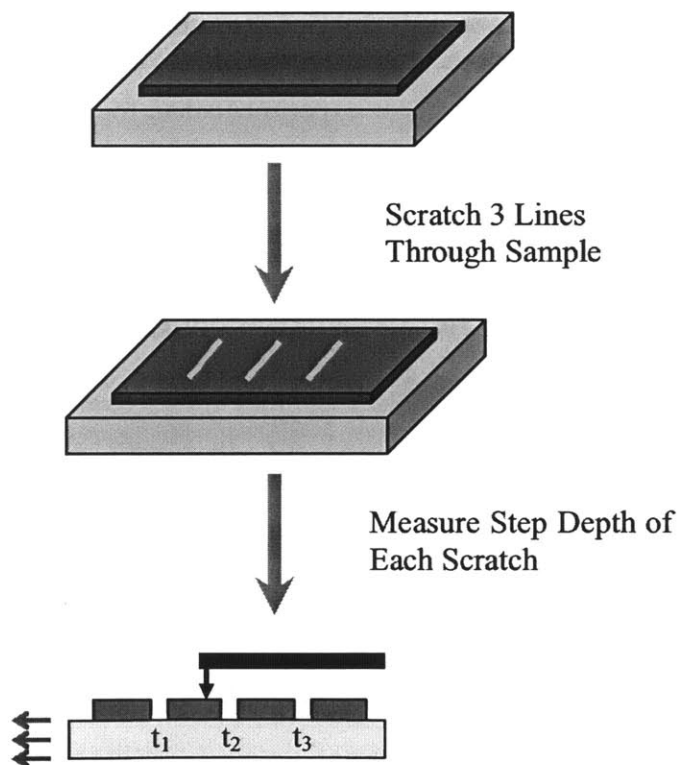
Figure 7: The process and locations of thickness measurements using the profilometer.

These three values were averaged using Equation 10 to obtain the estimated thickness of the sample. As can be seen, the estimated thickness is weighted towards the center thickness and is not just a simple average. This weighted average was performed so that a more accurate measurement of the thickness could be obtained in the area where electrical conductivity measurements were taken. The estimated thickness was used for the thickness (t) variable in the four-point electrical conductivity measurements (Eq. 8).

$$Estimated\ Thickness\ (t) = \frac{\left[\frac{(t_1+t_3)}{2}\right]+t_2}{2} \qquad \text{(Eq. 10)}$$

To obtain a more accurate electrical conductivity measurement, five electrical conductivity measurements were taken near the center of the sample (Figure 8). These five measurements were averaged together to develop the reported electrical conductivity of the sample.
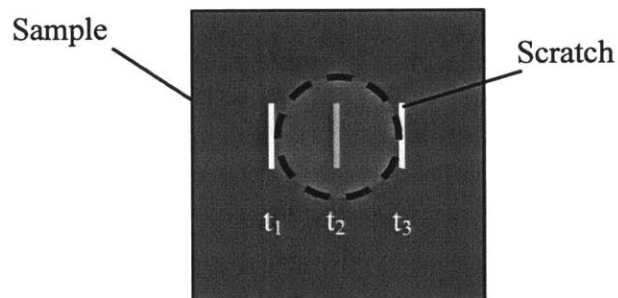
Figure 8: The electrical conductivity measurement area of the sample. The dotted circle represents the area where all five electrical conductivity measurements were taken.

2.1.3 Seebeck Coefficient (S)

The Seebeck coefficient (S) of all samples was measured with a homemade setup. Looking at Equation 6, in order to determine the Seebeck coefficient, it was necessary to induce a temperature gradient across the sample and measure the voltage drop (ΔV) and temperature difference (ΔT). To accomplish this, we built a Seebeck measurement device (Figure 9). The device used two commercially available peltier heaters (TE Technology, Inc.) to heat up one side of the sample and cool down the opposite side. Current was run through the peltier heaters in opposite directions using a current source (Keithley 2400), which made one device a heater and the other a cooler. Under each peltier heater/cooler was a small heatsink to help conduct heat and create the largest possible temperature difference across the heater or cooler. The sample and substrate bridged the gap between the heater and cooler.
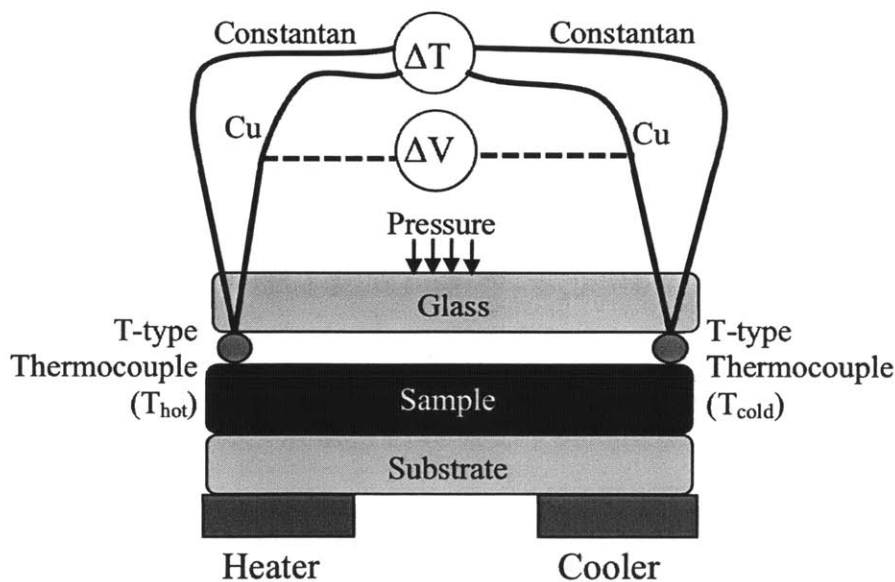
Figure 9: Schematic of Seebeck measurement device. The peltier heaters provide a temperature gradient across the sample. The temperature and voltage is measured by two T-type thermocouples. Pressure is provided on the thermocouples to maintain good electrical and thermal contact with the sample.

On each side of the sample was a T-type thermocouple (Omega, 5TC-TT-T-40-36) to measure the temperature and voltage on the hot and cold sides. Thermocouples, as opposed to other temperature measurement devices, were used in this setup because of their ability to measure both temperature and voltage, as well as their availability in very small sizes. The small size of the thermocouples, in this case 0.08 mm diameter, allowed them to reach steady state temperature quickly and gave us a more accurate measurement of the temperature of the sample. T-type thermocouples were specifically used in our setup for two reasons. First, they had high accuracy in our desired temperature range (~40 uV/K) and a small limit of error (1°C). Secondly, the copper leg of a T-type thermocouple junction had a very small Seebeck coefficient, which created a smaller error in the voltage measurement across the sample (Eq. 11).

The information from the thermocouples was collected by a data acquisition system (TC-08) connected to a computer with software (TC-08 Recorder). The thermocouples were connected to two separate inputs on the data acquisition system for direct temperature measurement of each side of the sample. To measure the voltage drop across the sample, additional copper wires were attached to the existing copper leads of the two thermocouples and connected to a separate input on the data acquisition system (Figure 9). The copper leg of the cold side thermocouple was connected to the positive input on the data acquisition system, and the copper leg of the hot side thermocouple was connected to the negative input. Therefore, a p-type material would register as having a positive voltage in the collected data. The copper legs of the thermocouples were used for measuring the voltage because they did not have a large Seebeck coefficient and produced a more accurate voltage measurement (Eq. 11). But even though there was not much error in the voltage measurements, the extra voltage induced in the

copper wires was removed during our data analysis. A schematic of the overall voltage measurement circuit can be found in Figure 10. The voltage measured by the data acquisition system was the sum of the voltage generated in the sample (what we want to know) and the voltages generated in the copper wires. Equation 11 shows the summation of these voltages. In order to find the voltage drop across the sample, we had to subtract the voltages generated within the copper wires. The copper wire voltages were calculated using the Seebeck coefficient of the copper wire, as well as the temperature at each junction (Figure 10). The temperature at the two sample junctions (2,3) was defined by the thermocouple measurements at each location. The temperature at data acquisition system junctions (1,4) was determined by a temperature measurement device located within the data acquisition system. Lastly, the Seebeck coefficient of the copper wire was assumed to be the same as that of bulk copper with values found from literature.[17] Since the Seebeck coefficient of copper changes with temperature, the value at each measurement was linearly interpolated using the literature values. In our setup, the voltages created by the copper wires underestimated the voltage drop across the sample.
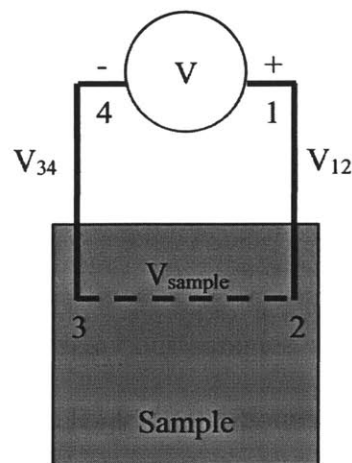
Figure 10: Overall voltage circuit of the Seebeck measurement device. The voltage induced in the copper wires (V_{12} and V_{34}) must be subtracted from the circuit in order to measure the Seebeck voltage of the sample (ΔV).

$$V_{measured} = V_{34} + V_{sample} + V_{12}$$

$$V_{measured} = [S_{Cu}(T_4 - T_3)] + [S_{sample}(T_3 - T_2)] + [S_{Cu}(T_2 - T_1)]$$

(Eq. 11)

The thermocouples used in our Seebeck device were twisted at the temperature measurement junction. This was done to avoid any voltage generated across a standard "v-style" junction on the sample. Figure 11 illustrates the difference between a "v-style" junction and a twisted junction. The "v-style" junction creates a circuit that includes a small length of the sample between its legs. If there was a temperature drop across this portion of the sample, then a voltage would be generated and measured by the thermocouple. This could cause the thermocouple to produce an inaccurate temperature measurement. By twisting the thermocouples, the small length of sample previously included in the circuit was eliminated, thereby producing a more accurate measurement of temperature.
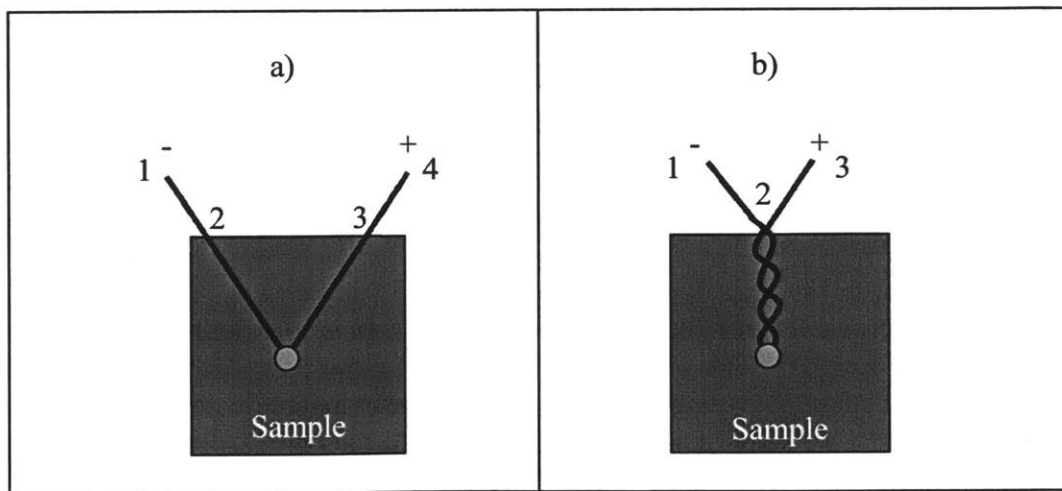
Figure 11: Illustration showing the difference between the (a) "v-style" thermocouple junction and (b) twisted thermocouple junction. The "v-style" junction will measure the voltage from the

positive leg (1-2), sample (2-3), and negative leg (3-4). The additional sample voltage (2-3) will cause inaccurate temperature measurements. The twisted junction avoids measuring any voltage generated within the sample between the positive and negative leg.

A glass microscope slide was clamped on top of the thermocouples to (a) ensure a good connection with low resistance between the sample and the thermocouples and (b) to insulate the top surface and reduce convection losses. Pressure was provided on the top surface of the microscope slide with a hold-down toggle clamp (McMaster-Carr, 5126A33). Since the clamp had a precise "closed" position, it allowed us to maintain a similar pressure across comparable samples. The glass cover also insulated the topside of the sample and thermocouples from any convective heat losses, which allowed for a more steady temperature and voltage measurements.
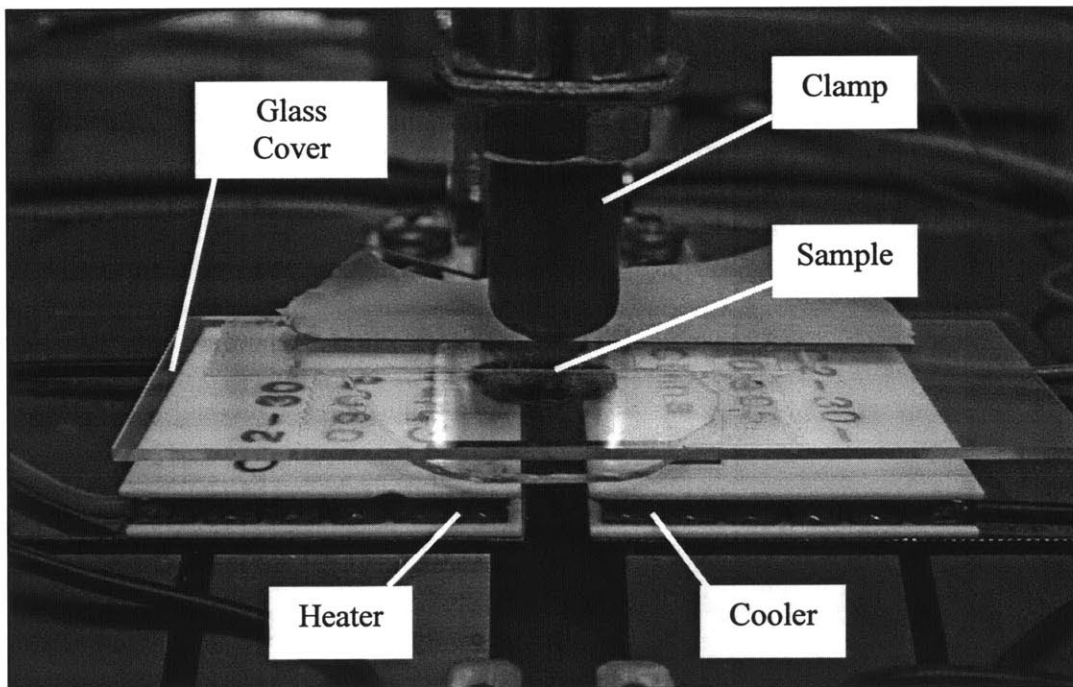
Figure 12: Close-up view of the Seebeck coefficient measurement device. The black pieces under the heater and cooler are heat sinks.

The Seebeck coefficient of each sample was calculated as the slope of the least squares fit line when plotting voltage drop (ΔV) against temperature gradient (ΔT) (Figure 13). First, the sample was loaded into the Seebeck device as shown in Figure 9. With no temperature difference applied to the sample (no current supplied to the peltier heaters), the steady state temperature and voltage was measured for about 5 seconds (1 measurement/sec). Then, the current through the peltier heater circuit was increased to 0.1 amps and the temperature/voltage measurements were allowed to reach steady state. This took about 95 seconds (sampling at 1 measurement/sec). Next, the current through the peltier heater circuit was increased to 0.2 amps and the temperature/voltage measurements were allowed to reach steady state. This took another 100 seconds (1 measurement/sec). Subsequently, the current through the peltier heater circuit was increased a third time to 0.3 amps and the temperature/voltage measurements were allowed to reach steady state. This took about another 100 seconds (1 measurement/sec). The data was then exported to Microsoft Excel for analysis. First, the temperature gradient for all measurements was calculated by subtracting the cold side temperature from the hot side temperature. Then, all of the measured voltages were corrected for the generated copper wire Seebeck voltages (Figure 10, Eq. 11). Next, the last 10 measurements (10 seconds) of voltage and temperature taken at each steady state temperature plateau were averaged together, which resulted in three points plotted as voltage drop (ΔV) versus temperature gradient (ΔT). The linear least squares fit of the three points was reported as the Seebeck coefficient of the sample.

For all silicon substrate samples, the temperature difference created using the current values mentioned above (0.1, 0.2, 0.3 amps) was not large enough. This was due to the high thermal conductivity of the silicon substrate. In order to create larger temperature gradients in the samples, current values of 0.2, 0.4, and 0.6 amps were used instead.

a)

Temp. Gradient (-ΔT)

10 sec

ΔT

ΔV

Plateau 1

Plateau 2

Plateau 3

Voltage (ΔV)

5   100   200   300

Time

b)

Voltage (ΔV)

Avg. of Plateau 3

Avg. of Plateau 2

Avg. of Plateau 1

Slope = -ΔV/ΔT = Seebeck

Temp. Gradient (-ΔT)
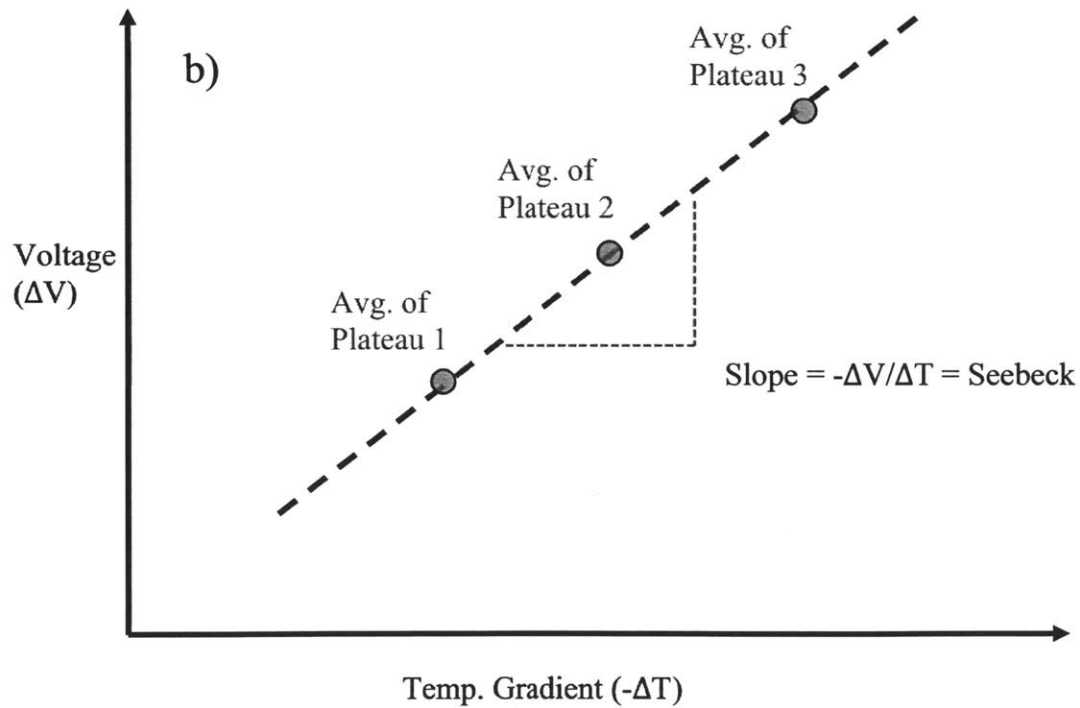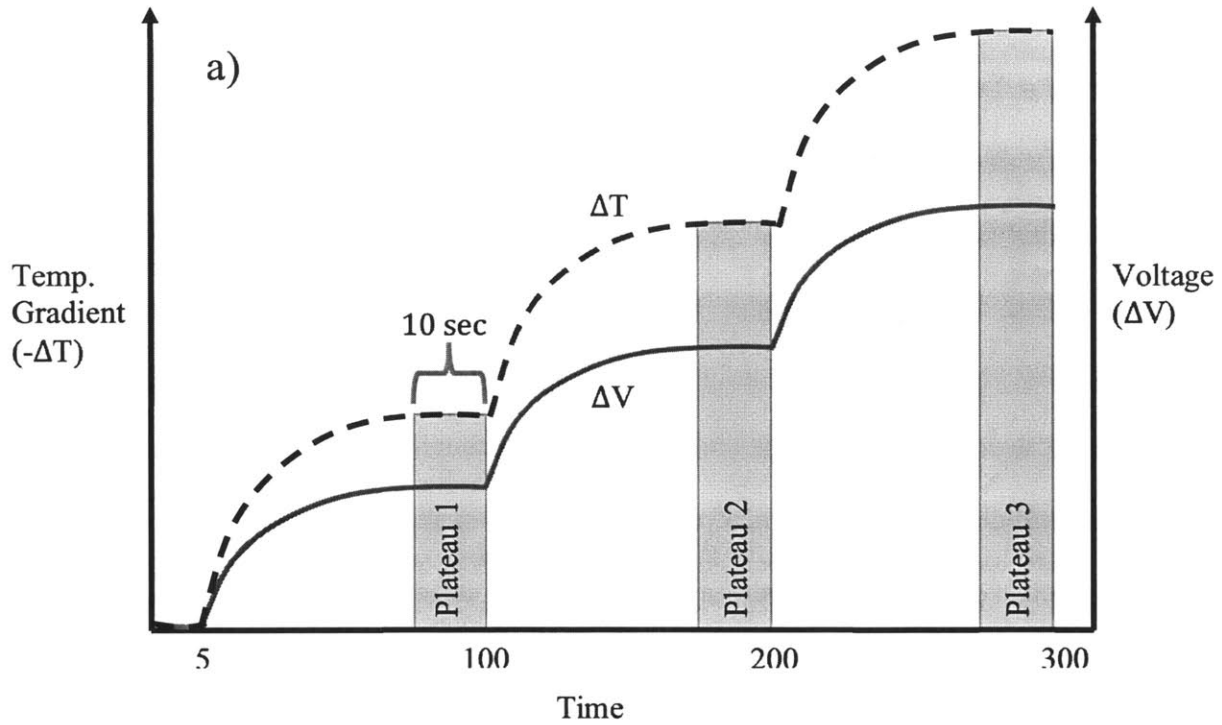
Figure 13: Data analysis process of Seebeck coefficient. (a) The average of voltage difference and temperature gradient were taken at each plateau and (b) plotted to find the linear least squares fit. The slope of the least squares fit was reported as the Seebeck coefficient of the sample.

The accuracy of our Seebeck device was checked using a nickel substrate because it had been used in previously published literature and had well known Seebeck values near room temperature (~ -19.4uV/K @ 300K).[18] The nickel substrate (99.98%, 357553-2.8G, Sigma-Aldrich) was measured three times in three different positions in the Seebeck device. The averaged value was -18.97 uV/K with a standard deviation of 0.32 uV/K. Our average differed by only 2.2% from the literature value, which confirmed the operation and accuracy of our Seebeck device.

2.1.4 Mean Temperature (T_m)

The mean temperature (T_m) of our property measurements was always near room temperature (~ 25°C, 298 K). The mean temperature is defined as the average temperature between the hot side and cold side of the thermoelectric device during operation. In our Seebeck measurements, the mean temperature can be extracted by taking the average between the hot side and cold side temperature measurements. For the electrical conductivity measurements, the mean temperature was the temperature of the room. For all of our electrical conductivity and Seebeck coefficient measurements, the mean temperature stayed between 22°C and 29°C. Since the research of this thesis was focused on maximizing the Seebeck coefficient and electrical conductivity, the dimensionless figure of merit was not calculated and the mean temperature for each measurement was not recorded.

2.2 Measurement Procedure

The samples created in this research utilized two different methods of deposition (dropcasting or spin coating) and three different types of substrates (glass slide, glass coverslip, or silicon substrate). Regardless of the sample, the overall procedure used for obtaining results involved three steps: (1) material preparation, (2) sample creation, and (3) property measurement.

2.2.1 Material Preparation

Conductive polymer PEDOT:PSS (Clevios PH1000) was purchased from Heraeus and stored in a dark refrigerator at 5-10 °C per the manufacturers specifications. To make the polymer more conductive, it was combined with solvent dimethyl sulfoxide (DMSO, Sigma-Aldrich, D8418) in a small glass scintillation vial. The amount of DMSO (measured in weight percent) combined with PEDOT:PSS was measured using the aqueous density of PEDOT:PSS (1 g/mL) and the liquid density of DMSO (1.1 g/mL). After combining the materials, the mixture was sonicated for 15 minutes. For spin coated samples, ethanol (200 Proof, Koptec) was added to the polymer mixture and sonicated for another 15 minutes. Mixtures were stored inside a dark refrigerator at 5-10 °C until used for sample deposition.

2.2.2 Sample Creation

All samples in this research were created by dropcasting or spin coating onto glass slides, glass coverslips, silicon substrates, or silicon-on-insulator (SOI) substrates. Glass microscope slides (VWR, Item 16004-368) were cut to 25mm x 25mm square size for sample deposition. Glass coverslips (Ted Pella, Item 26024) were round with a 15mm diameter. The silicon

substrates (MTI) were 10mm x 10mm x 0.5mm undoped silicon with <100> orientation and one-side polished. The SOI substrates (ACA Technology, Inc.) were about 20mm x 20mm square. They had a 50nm device layer of undoped single crystal silicon on top of 375nm SiO_2 supported by about 5um of undoped Si. The SOI wafer allowed us to experiment with a very thin layer of silicon (50nm).

All glass slides and coverslips were cleaned using the follow methodology: (1) sonicated 15 minutes in Acetone, (2) sonicated 15 minutes in methanol, (3) sonicated 15 minutes in DI water. Glass slides were dried in an oven at 110 °C for 45 minutes (Carbolite CWF 1300). Glass coverslips were dried with compressed nitrogen gas. To remove the insulating oxide layer, silicon substrates and SOI substrates were submerged in hydrofluoric acid (4.4 wt.%) for 60 seconds, then rinsed by submerging in DI water for 5 seconds and rinsed again by submerging in a different container of DI water for another 5 seconds. The substrates were then spin coated within 30 seconds to keep oxide layer formation to a minimum.

Dropcasting was performed for all samples created during the first section of the results of this thesis (Section 3.1). First, PEDOT:PSS and DMSO were combined into scintillation vials at varying weight percentage ratios. Then, the mixtures were sonicated in a water bath for 15 minutes to homogeneously mix the constituents. Using a micropipette, 0.1 mL of the mixtures was then dropcast onto clean glass slides and samples were dried (Carbolite CWF 1300) for 4 hours at 50 °C and 15 minutes at 120 °C. Sample thickness varied from 3 to 10 um.

Spin coating (SCS 6800) was performed for thin film PEDOT:PSS samples on glass coverslips, PEDOT:PSS on silicon substrates, and PEDOT:PSS on SOI substrates (Section 3.2, 3.3). First, PEDOT:PSS and DMSO were combined into scintillation vials at varying weight percentage ratios. Then, the mixtures were sonicated in a water bath for 15 minutes to

homogeneously mix the constituents. Next, the mixtures were combined with varying volume ratios of ethanol and sonicated again for 15 minutes. The surface of the glass coverslip or polished side of the silicon substrate was completely covered with the PEDOT:PSS, DMSO, and ethanol mixture and spun at varying RPMs (rotations per minute) for 180 seconds with no ramp time.

2.2.3 Property Measurement

The properties of the samples were measured in the following order: electrical conductivity, Seebeck coefficient, and thickness. The electrical conductivity was measured first because a uniform, continuous PEDOT:PSS film produced the most accurate measurements. These initial measurements used a "guessed" thickness of each sample, which were then corrected using the actual estimated thickness after surface profilometry was performed. The Seebeck coefficient measurements and thickness measurements created divots and scratches in the PEDOT:PSS film, which is why they were performed after the electrical conductivity measurements. Furthermore, the Seebeck measurement was performed second in this process because a continuous film is needed to measure the voltage drop across the sample. The tiny divots created by the four-point probe conductivity measurements did not affect the Seebeck measurement, but the long scratches created for the thickness measurement could have caused inaccuracies. This is why the thickness measurement was performed last.

2.2.3.1 Measuring PEDOT:PSS on Si Substrate in the Dark

The electrical conductivity and Seebeck coefficient measurements of all PEDOT:PSS on silicon substrate samples were performed in the dark. It was discovered that the coating of PEDOT:PSS on a silicon substrate created a P-N junction, much like that of a photovoltaic cell. As light from the room hit the surface of the sample, electrons would become excited and produce large voltage measurements without any temperature gradient across the sample. To eliminate this issue, we performed the measurements in a room without windows, turned all the lights off, and covered the device with an opaque box. This environment was used for all electrical conductivity and Seebeck coefficient measurements of PEDOT:PSS coated silicon samples.

3 Results and Discussion

In order to investigate the thermoelectric properties at the interface of conductive polymer PEDOT:PSS and high-Seebeck undoped silicon, several hurdles had to be overcome. First, the electrical conductivity of PEDOT:PSS had to be shown to increase when mixed with solvent DMSO. Second, a method to create continuous thin films of PEDOT:PSS on the order of 10 nm thickness had to be devised using spin coating. And lastly, using these two methods, the thermoelectric properties at the interface of PEDOT:PSS and silicon could be investigated.

3.1 Enhanced Electrical Conductivity of PEDOT:PSS using DMSO

The electrical conductivity of conductive polymer PEDOT:PSS has been shown to increase dramatically with the addition of solvents.[4,13,14,19,20] We confirmed this increase in electrical conductivity using DMSO (Figure 14). Twelve samples (three at each wt.% DMSO) were created via dropcasting PEDOT:PSS onto glass slides with 0, 5, 10, and 15 wt.% DMSO. The thickness of these samples measured between 5 to 8 um, and the error bars were one standard deviation from the mean. PEDOT:PSS without any solvent had an electrical conductivity of 0.7 S/cm. The addition of just 5 wt.% DMSO to the solution increased the electrical conductivity to 633.6 S/cm. This increase in conductivity is similar to that found in a previously mentioned publication (Figure 5).[4] It appeared that the PEDOT:PSS became saturated at 5 wt.% DMSO as there was no significant change in the electrical conductivity at 10 wt.% DMSO or 15 wt.% DMSO. Since no noticeable change occurs at these increased amounts of DMSO, 5 wt.% DMSO was used on all further PEDOT:PSS thin film experiments. It was noticed that at 20 wt.% DMSO, the films become shriveled and nonuniform in thickness, making

the samples difficult to measure accurately. It should also be noticed that the Seebeck coefficient

of the PEDOT:PSS films shows only a slight decrease with the addition of DMSO, even up to 15

wt.% DMSO. As mentioned before, the cause for the increase in electrical conductivity and lack

of change in the Seebeck coefficient with the addition of DMSO is unclear (See Section 1.4).
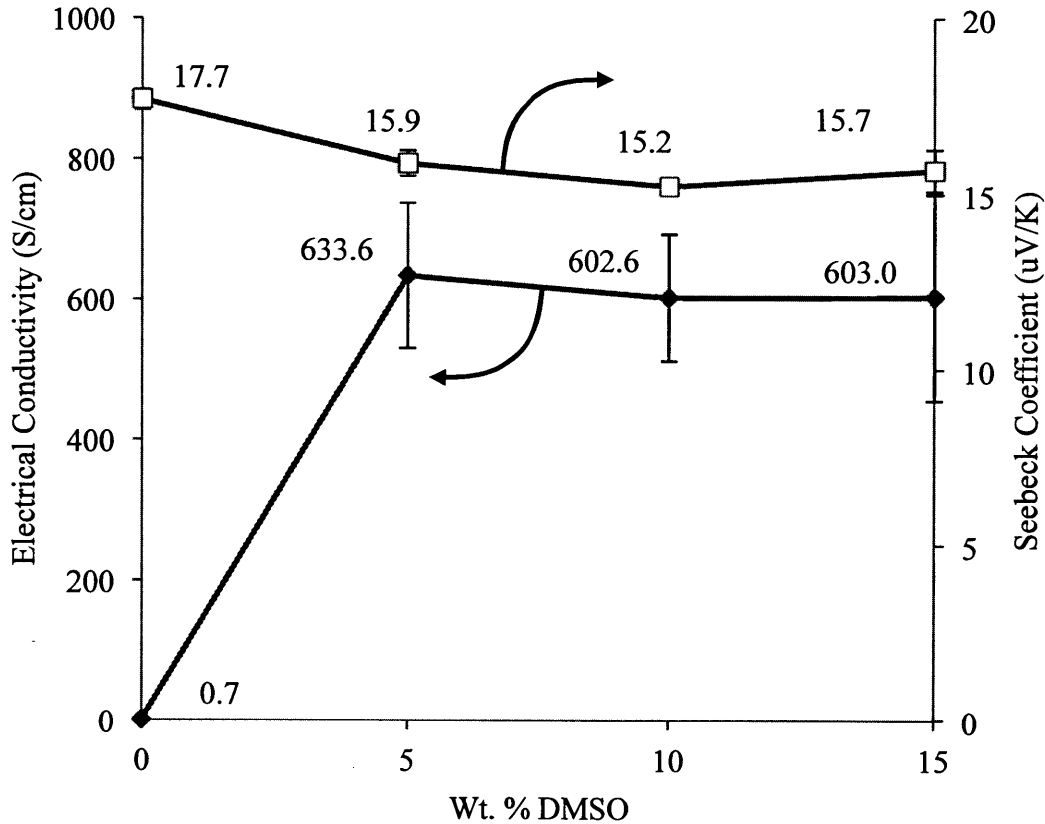

Figure 14: The electrical conductivity (◆) and Seebeck coefficient (□) of PEDOT:PSS films with the addition of solvent DMSO. The electrical conductivity increases significantly (almost three orders of magnitude) with just 5 wt.% DMSO. However, the Seebeck coefficient shows only a small decrease with the addition of DMSO. The error bars are one standard deviation from the mean.

3.2 Nanoscale PEDOT:PSS + DMSO Thin Films

In order to achieve nanoscale thin films of PEDOT:PSS on silicon substrates, we first devised a method to create nanoscale thin films on glass substrates using spin coating. This also allowed us to confirm that the electrical conductivity and Seebeck coefficient did not change significantly at very small thicknesses. First, it was noticed that spin coating PEDOT:PSS + 5 wt.% DMSO onto glass substrates resulted in non-uniform, discontinuous films (Figure 15a). It was thought that this was caused by the high surface tension of the polymer mixture (primarily water), which made it too hydrophobic to be spin coated uniformly. Films with a uniform thickness were needed to make accurate electrical conductivity measurements. To solve this issue, we added ethanol to decrease the surface tension of the mixture (Table 3).[21] The addition of ethanol made the mixture more hydrophilic on the glass substrate and allowed for a more uniform coating of the surface (Figure 15b-d).
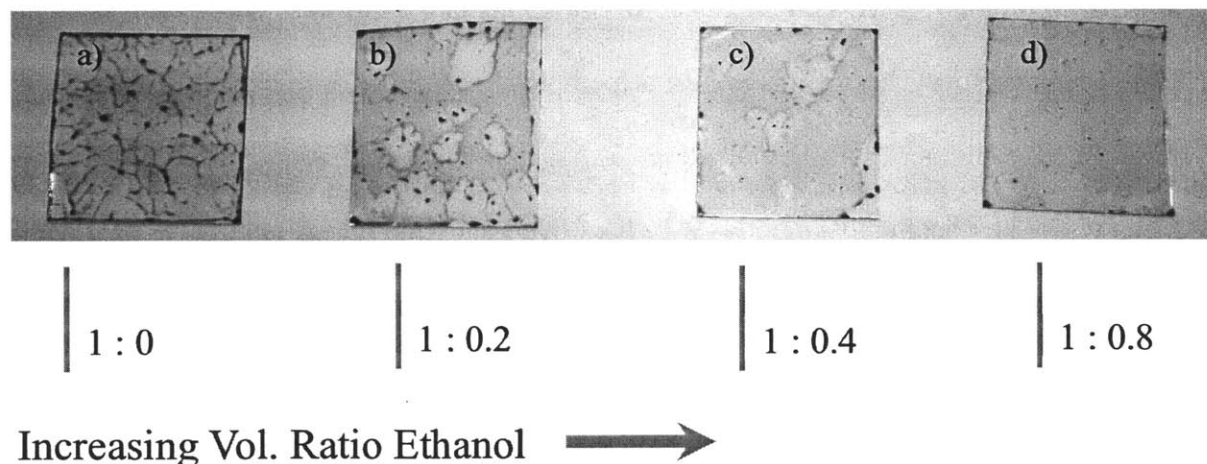

Figure 15: (PEDOT:PSS + 5 wt.% DMSO) mixture with increasing volume of ethanol. The ratios are (volume polymer mixture : volume ethanol). Adding ethanol to the polymer mixture allows for uniform coating of the surface via spin coating.

Volume Ratio (Water: Ethanol)	Mass % Ethanol	Surface Tension with Air @ 25C (mN/m)
(1:0)	0.0%	72.01
(1:1)	44.1%	29.3
(1:5)	79.8%	23.8

Table 3: Surface tension values of (water : ethanol) mixtures. Our polymer mixture is comprised mostly of water, which shows how dramatically the surface tension should be reduced upon the addition of ethanol. The reduction of surface tension made the polymer mixture more hydrophilic and created more uniform and continuous thin films when spin coated. The values of surface tension are from literature.[21]

It was also discovered that increasing the amount of ethanol reduced the thickness of the resulting film (Figure 16a). Using a volume ratio of 1:5 (PEDOT:PSS + 5 wt.%DMSO : ethanol) and a spin speed of 9000 RPM, a continuous thin film of about 3.3 nm was achieved on a 15 mm diameter glass coverslip. These films were not completely uniform in thickness, as the center was usually a little thinner than the outside area, but they were continuous. The continuity of these films was a key accomplishment as it proved that nanoscale thin films of PEDOT:PSS + 5wt.% DMSO could be achieved with spin coating.

The electrical conductivity and Seebeck coefficient of these thin films was also close to that of the thicker dropcast films (Figure 16b). The nanoscale samples maintained an average electrical conductivity of 424 S/cm and average Seebeck coefficient of 12 uV/K. These values were not far below the values of the thicker dropcast films using 5 wt.% DMSO, which were 634 S/cm and 16 uV/K, respectively. It was unclear why there was a small decrease in the thermoelectric properties of the nanoscale thin film samples. We believe this decrease may be

caused by the reduced number of chains making fewer electrical connections, which would have

a negative impact on the ability for electrons to travel through the film.
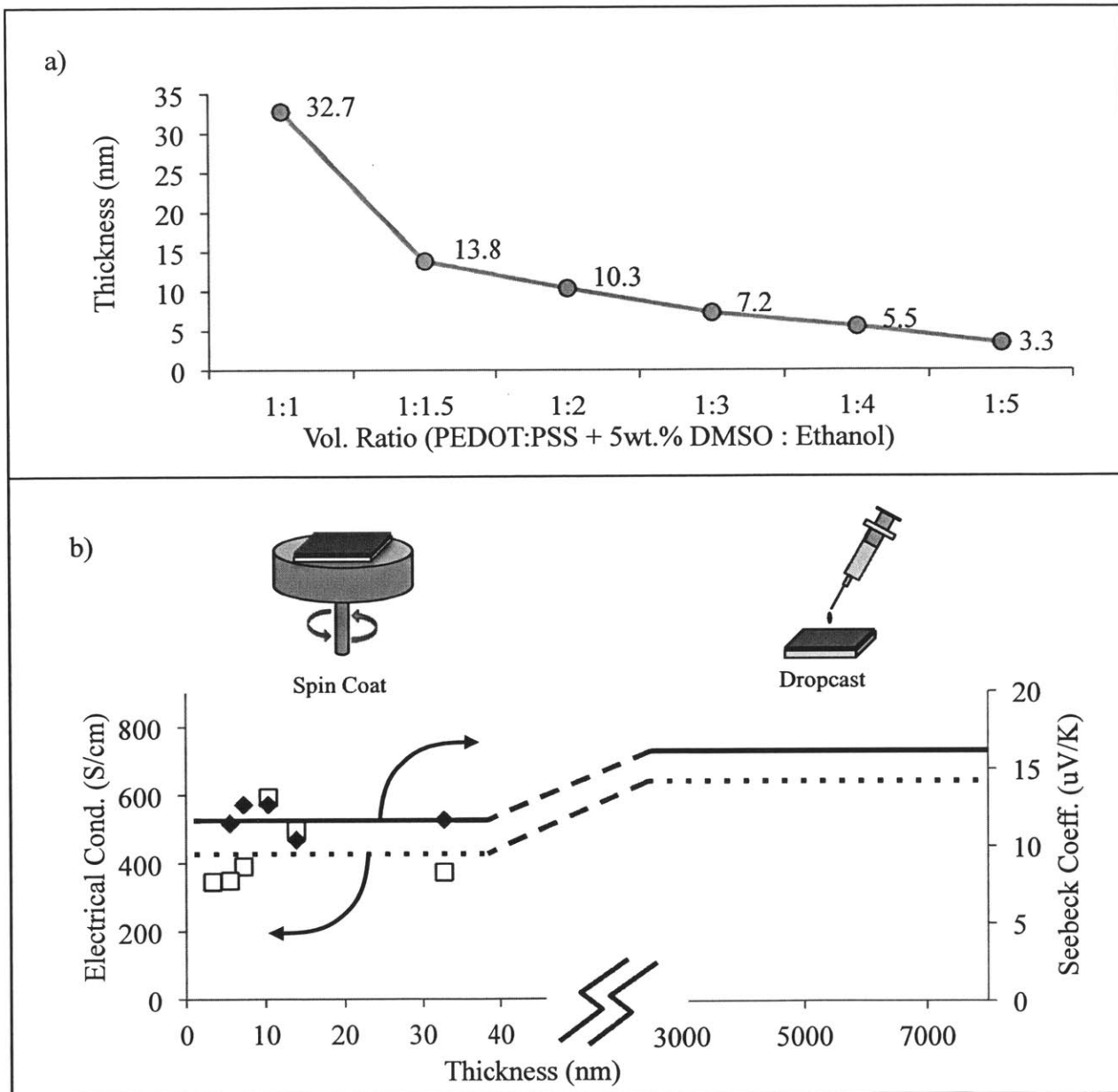
Figure 16: (a) Thickness of PEDOT:PSS film with increasing volume ratio of ethanol. Continuous films near 3.3 nm thickness were achieved with a 1:5 volume ratio of polymer solution to ethanol. (b) Electrical conductivity (□) and Seebeck coefficient (◆) of the thin PEDOT:PSS films with ethanol. The average electrical conductivity (dotted line) and Seebeck coefficient (solid line) of the nanoscale samples were slightly below that of the micron-scale samples. Data for right side of (b) was from Figure 14 at 5 wt.% DMSO. All spin coated samples were spun at 9000 RPM for 180 seconds.

3.3 Enhanced Seebeck Coefficient at Si / PEDOT:PSS Interface

To investigate any possible change in thermoelectric properties at the interface between silicon and PEDOT:PSS, we used the methodology gained from Section 3.2 to spin coat thin films of PEDOT:PSS onto hydrofluoric acid (HF) -etched undoped silicon substrates. Different thicknesses of PEDOT:PSS were placed on 5 um silicon substrates using a (1:5) volume ratio of (95 wt.% PEDOT:PSS + 5wt.% DMSO : ethanol) mixture and spin coating at speeds of 9000, 5000, 3000, 2000, and 1000 RPM. A total of 6 samples were made (one at each data point), and the error bars are one standard deviation from the mean. The results revealed that there was an interface interaction between the two materials that caused an increased Seebeck coefficient (Figure 17). Unmodified, the silicon substrate had an electrical conductivity of 0.00038 S/cm and a Seebeck coefficient of -1272 uV/K. Upon the addition of thin layers of PEDOT:PSS, the Seebeck coefficient at the interface of the two materials became significantly more positive, reaching a maximum of 468 uV/K with a PEDOT:PSS thickness near 13.5 nm. It was also noticed that the electrical conductivity increases with the thickness of the PEDOT:PSS layer to a maximum of 0.0012 S/cm with a 21.75 nm thickness.

Electrical Conductivity (S/cm)

0.002

0.0015

0.001

0.0005

0

Seebeck (uV/K)

600

400

200

0

-200

-400

-600

-800

-1000

-1200

-1400

0   5   10   15   20   25

Estimated Thickness of PEDOT:PSS Layer (nm)
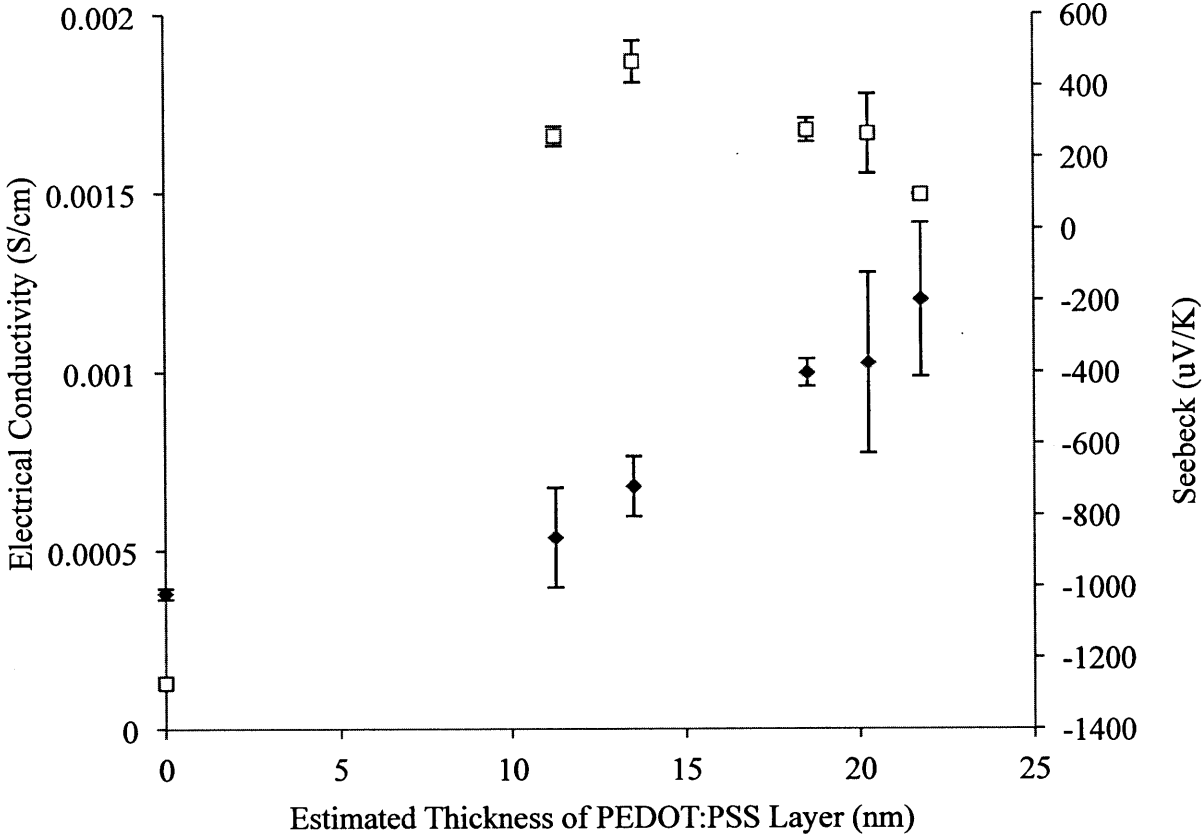
Figure 17: Electrical conductivity (◆) and Seebeck coefficient (□) of PEDOT:PSS on 500 um silicon substrate. Increasing the thickness of PEDOT:PSS resulted in increased electrical conductivity values at the interface. The addition of PEDOT:PSS also created an enhanced p-type Seebeck coefficient at the interface with a maximum value of 468 uV/K with a 13.5 nm thick PEDOT:PSS film. Error bars are one standard deviation from the mean.

The electrical conductivity from Figure 17 was calculated using the full thickness of the silicon substrate (500 um) combined with the thickness of the PEDOT:PSS film (11-22 nm). Using the full thickness of the silicon substrate is probably not an accurate depiction of the electrical conductivity at the interface, but it did create the most conservative estimation and allowed the overall increasing trend to be seen. However, to confirm whether the full 500 um of silicon was necessary to change the thermoelectric properties, or if the observed trends are in fact just an interface effect, we used the same experimental procedure to spin coat PEDOT:PSS onto

50 nm device layer SOI substrates (Figure 18). This allowed us to investigate the thermoelectric

properties at the interface between the thin PEDOT:PSS layer and 50 nm of undoped silicon.
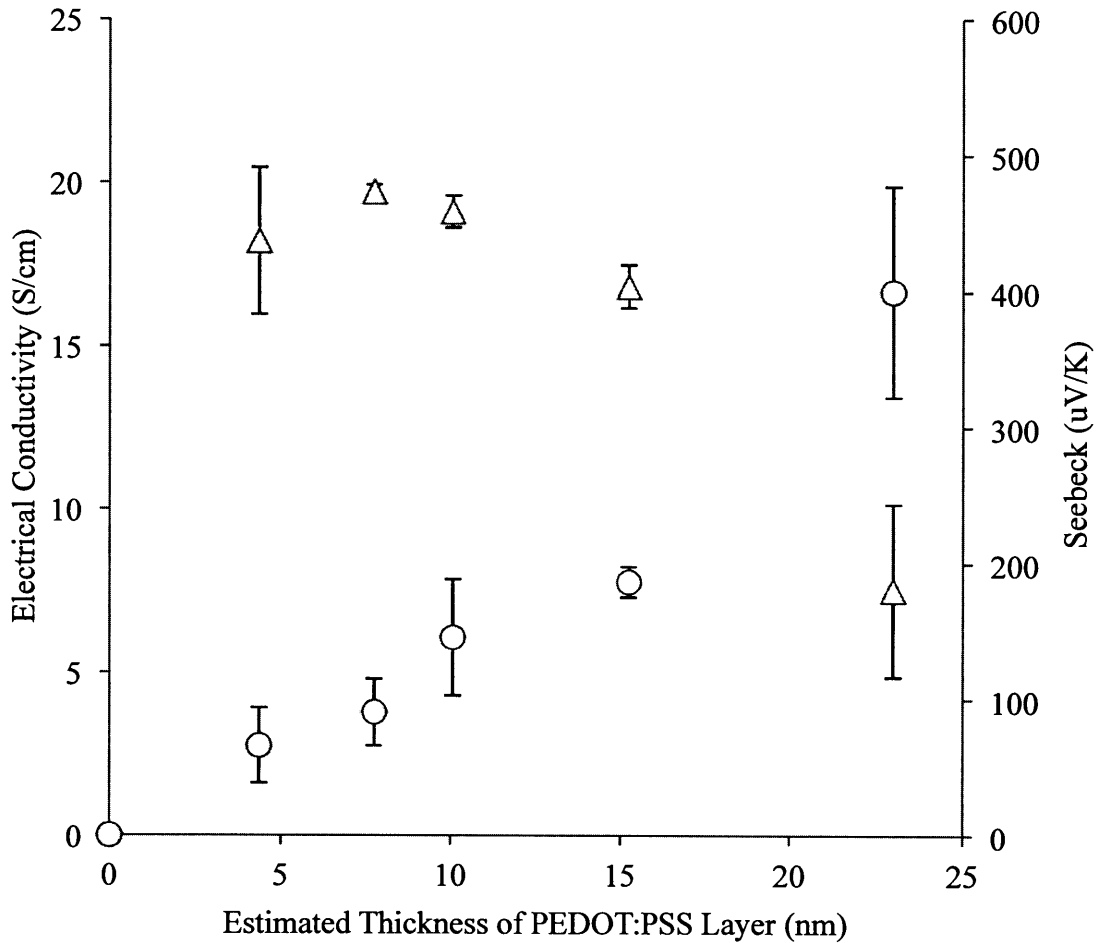
Figure 18: Electrical conductivity (O) and Seebeck coefficient (Δ) of PEDOT:PSS on 50 nm SOI substrate. Increasing the thickness of PEDOT:PSS resulted in increased electrical conductivity values at the interface. The addition of PEDOT:PSS also created an enhanced p-type Seebeck coefficient at the interface with a maximum value of 473 uV/K with a 7.75 nm thick PEDOT:PSS film. The bare SOI substrate had an electrical conductivity of 0.00027 S/cm, but the Seebeck coefficient could not be measured. Error bars are one standard deviation from the mean.

The Seebeck coefficient of the bare 50 nm SOI (zero thickness of PEDOT:PSS) substrate

could not be measured because the sample was too resistive. However, upon adding a thin

PEDOT:PSS layer, the results showed that the enhancement in the Seebeck coefficient still

existed using the 50 nm SOI substrates (473 uV/K with 7.75 nm PEDOT:PSS layer). The electrical conductivity, on the other hand, showed a dramatic improvement over the 500 um samples. We believed this enhancement was due to the fact that a much smaller thickness of silicon (50 nm vs 500 um) was used in the overall measurements. To eliminate the thickness dependence when comparing the electrical conductivity between the 500 um substrates and 50 nm SOI substrates, we instead compared their sheet resistance values (Figure 19). The sheet resistance measurements were just the resistance that was measured by the electrical conductivity device (LucasLabs Pro4) during our typical measurement procedure.
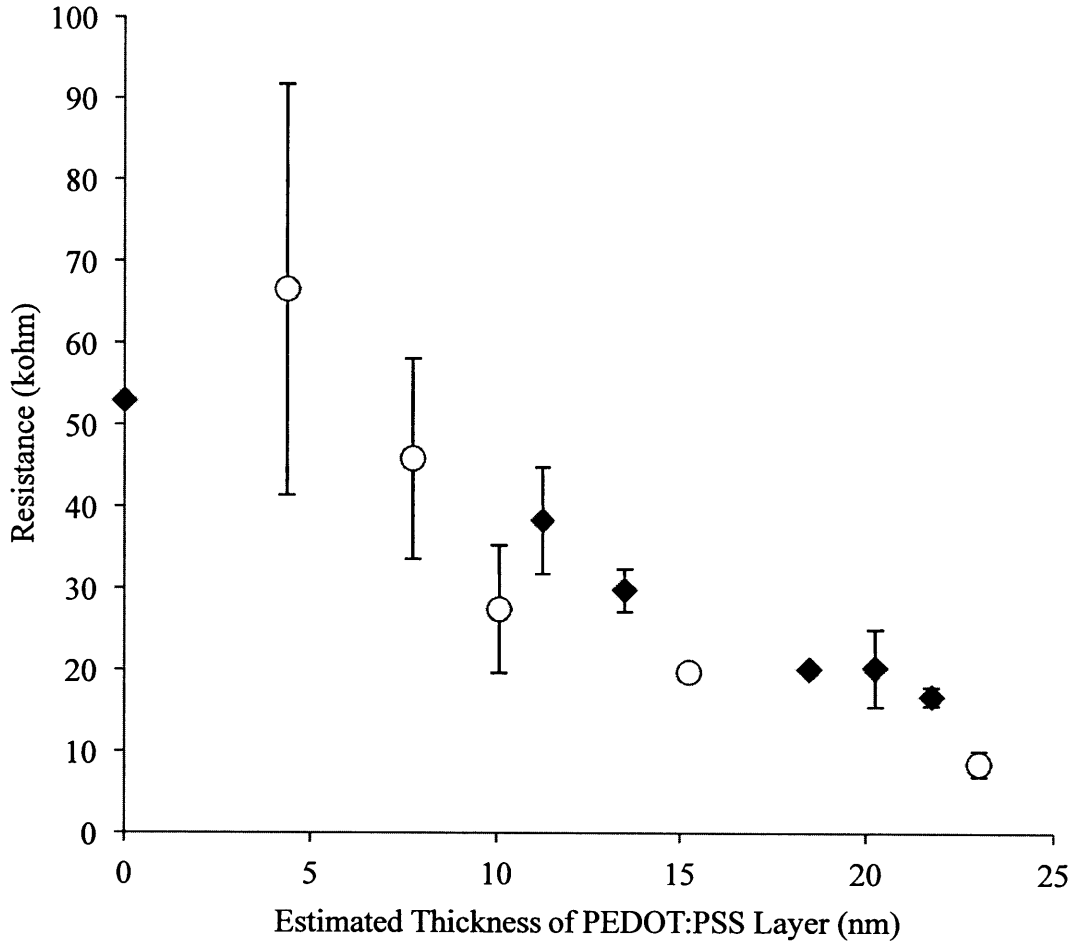
Figure 19: Comparison of the electrical sheet resistance of the 500 um silicon substrate samples (◆) and the 50 nm SOI substrate samples (O). Increasing the thickness of PEDOT:PSS resulted in a reduced sheet resistance (increased conductivity) at the interface. The values between both sample types were similar, which provided evidence that the thermoelectric property interaction was localized to the interface. The sheet resistance of the bare 50 nm SOI substrate was 7.4×10^8 ohms and is not shown in the graph. Error bars are one standard deviation from the mean.

These results showed similar sheet resistance values between the 500 um samples and the 50 nm SOI samples, which provides evidence of similar electrical conductivities at the interface between both types of substrates. Furthermore, since the electrical sheet resistance and Seebeck coefficient between the samples using both 500 um and 50 nm SOI substrates were similar, it confirmed our belief that the enhancement of the Seebeck coefficient and change in electrical conductivity are occurring at the interface between PEDOT:PSS and undoped silicon.

The increase in electrical conductivity with increasing PEDOT:PSS thickness was expected. Since both silicon substrates were highly resistive, the addition of highly conductive PEDOT:PSS was expected to increase the overall conductivity near the interface. This enhancement appeared to be similar to a bulk mixing effect as the electrical conductivity never exceeded the value of PEDOT:PSS and never fell below the value of the silicon. It was also noticed that the interface did not function as two resistors in parallel because the measured resistance was in between the values measured for the silicon substrates and PEDOT:PSS individually.

The increase in the Seebeck coefficient to a value more positive than that of inherent PEDOT:PSS proved that there was an interaction taking place at the interface of the two materials. Since the pristine undoped 500 um silicon substrate showed a negative Seebeck coefficient, it probably had some minor impurities causing it to become an n-type semiconductor. The Seebeck coefficient of PEDOT:PSS, on the other hand, had a positive Seebeck and could be considered a p-type semiconductor. Therefore, the interface between the two materials formed a P-N junction, a phenomenon that has been reported in previous literature.[22] The P-N junction created band bending at the interface, which made it sensitive to light and necessitated doing all measurements in the dark (Section 2.2.3.1). The p-type Seebeck coefficient enhancement to a value above that inherent to PEDOT:PSS and current thermoelectric materials proved that the interaction was not just a "mixing" of properties (Figure 20a). This increase could be explained by a bulk diffusion of charge carriers at the interface of the materials (Figure 20b). First, as a p-type material, the PEDOT:PSS had an excess of positive charge carriers (holes). The silicon, as an n-type material, had a deficiency of positive charge carriers. The interface of these two materials allowed the excess positive charge carriers to diffuse from the PEDOT:PSS to the

silicon substrate. This reduced the carrier concentration (n) near the interface of the two

materials causing an increase in the Seebeck coefficient (Eq. 7). It should also be noted that the

Seebeck coefficient shows a peak value on both substrates when using a PEDOT:PSS thickness

between 7 nm and 14 nm. These peaks indicate that the Seebeck coefficient could be optimized

using the thickness of PEDOT:PSS as a variable, but also that measuring the properties at the

interface becomes more difficult with a thick layer of PEDOT:PSS.
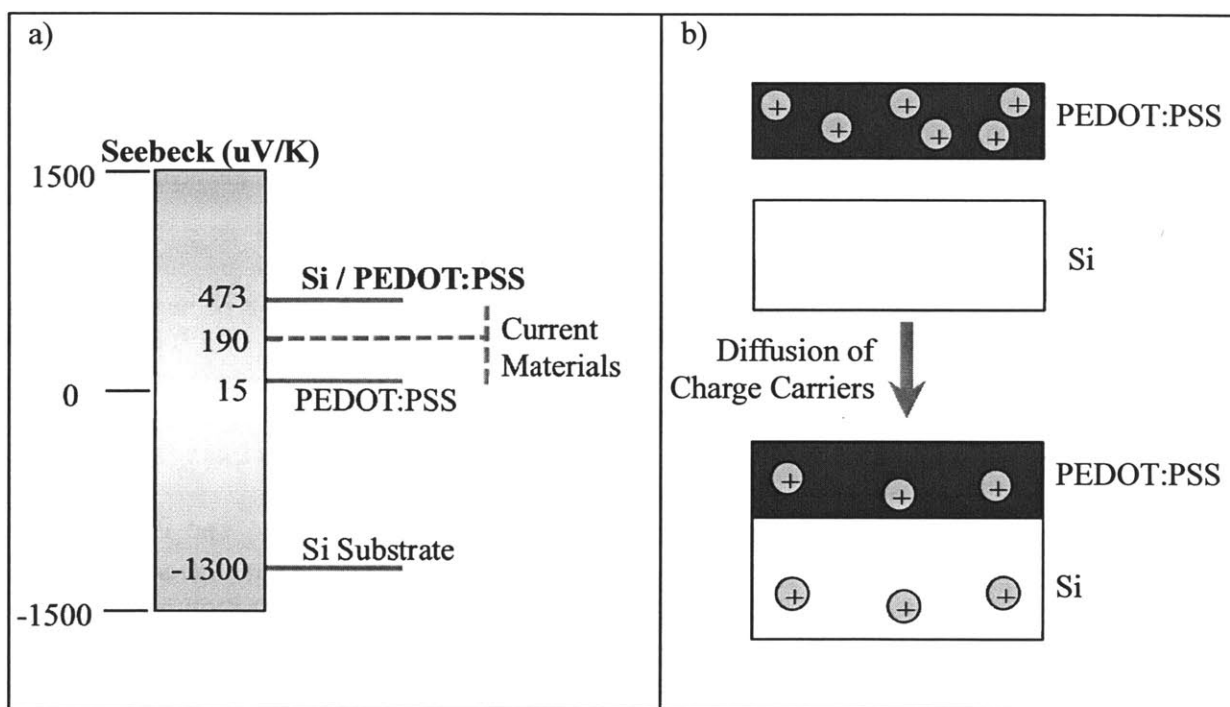
Figure 20: (a) The Seebeck coefficients of PEDOT:PSS, Si, Si / PEDOT:PSS interface, and current state-of-the-art BiSbTe semiconductor thermoelectric materials. The Si / PEDOT:PSS interface exhibits a Seebeck coefficient exceeding that of modern thermoelectrics (Table 1). (b) The enhancement of Seebeck coefficient may have been due to the diffusion of charge carriers away from the interface, which reduced the carrier concentration (n) near the interface.

In thermoelectric material research, it is common to calculate the power factor of a

material in order to optimize its properties in the dimensionless figure-of-merit (Eq. 3). The

power factor ($S^2\sigma$) is the product of the electrical conductivity with the square of the Seebeck coefficient and can be seen in the numerator of the dimensionless figure-of-merit (Eq. 3). The power factor of the PEDOT:PSS coated 50 nm SOI substrate samples are shown in Figure 21. A clear trend is seen in the data with a peak of 1.24 uW/K^2-cm occurring at a PEDOT:PSS thickness of 15.25 nm. The results from these experiments have shown the ability to significantly enhance the Seebeck coefficient of PEDOT:PSS at the interface with undoped silicon. Furthermore, we have shown that the power factor of the interface can be optimized by varying the thickness of the PEDOT:PSS layer.
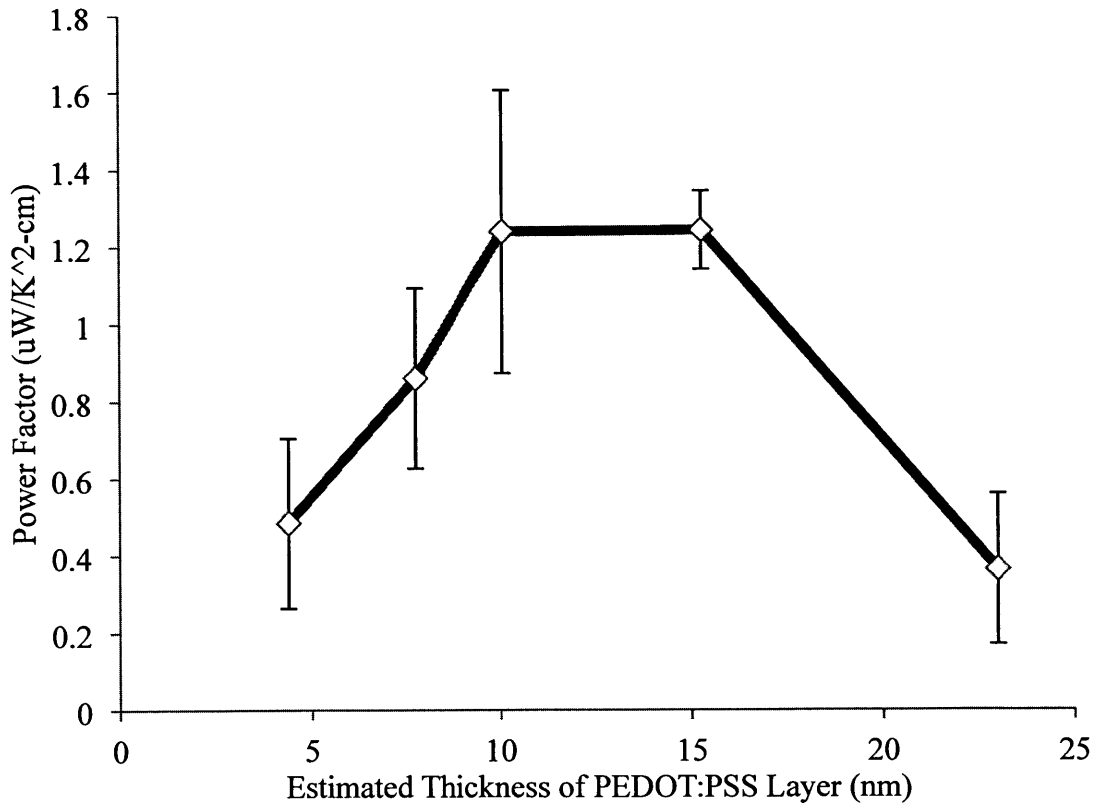

Figure 21: The power factor of 95 wt.% PEDOT:PSS + 5 wt.% DMSO coated on 50 nm SOI substrates. The power factor reaches a maximum of 1.24 uW/K^2-cm with a PEDOT:PSS thickness of 15.25 nm.

4 Conclusions and Future Work

In this work, we have shown (1) the successful construction and calibration of a thin film Seebeck measurement device, (2) the enhancement of electrical conductivity of PEDOT:PSS with the addition of DMSO and methodology to create conductive thin films of down to ~3 nm, and (3) the ability to enhance the Seebeck coefficient of conductive polymer PEDOT:PSS at the interface with undoped silicon.

4.1 Seebeck Measurement Device

The Seebeck measurement device we have created in this research is suitable for measuring thin film materials and has been successfully calibrated to within 2.2% of published values for nickel metal. This device is an efficient and accurate way to provide a temperature gradient and measure both temperature difference (ΔT) and voltage difference (ΔV) at two different points on the surface of a sample. Due to the softness and malleability of PEDOT:PSS thin films, the junctions of our thermocouples could penetrate the PEDOT:PSS and make contact with both the substrate and the PEDOT:PSS film. This was effective for measuring properties at the interface of the PEDOT:PSS / Si samples.

4.2 Electrical Conductivity Enhancement of PEDOT:PSS with Addition of DMSO and Creation of Nanoscale Thin Films

The electrical conductivity of PEDOT:PSS was shown to increase with addition of 5 wt.% DMSO from 0.7 S/cm to 633.6 S/cm. This enhancement in conductivity resulted in only a

small decrease of the Seebeck coefficient from 17.7 uV/K down to 15.9 uV/K. Using this mixture of PEDOT:PSS and DMSO, we also created conductive nanoscale thin films of PEDOT:PSS via spin coating down to ~ 3nm thick on glass substrates. The aqueous polymer mixtures were combined with ethanol in order to reduce the surface tension and make the mixture more hydrophilic on the surface of the glass slide. The thickness of the deposited PEDOT:PSS layer could be controlled by varying the volume fraction of ethanol and spin speed. The nanoscale thin films showed a small decrease in both electrical conductivity and Seebeck coefficient compared to that of the thicker dropcast PEDOT:PSS samples with values of of 424 S/cm and 12 uV/K, respectively.

4.3 Enhanced Seebeck Coefficient at Si / PEDOT:PSS Interface

The results from this research have shown that it is possible to enhance the Seebeck coefficient of conductive polymer PEDOT:PSS at the interface of undoped silicon. Moreover, the enhancement of the Seebeck coefficient appeared to be caused by interface interactions between the two materials because the phenomenon was shown to exist using both 500 um thick silicon and a 50 nm thick silicon. The highest Seebeck coefficient achieved at the interface was 473 uV/K with a 7.75 nm PEDOT:PSS film thickness. This value is higher than that of modern thermoelectric BiSbTe alloys (Table 1). Unfortunately, the electrical conductivity measured for this sample (3.78 S/cm) was much lower than modern thermoelectric materials and was indeed much lower than thin film 95 wt.% PEDOT:PSS + 5 wt.% DMSO alone (~ 400 S/cm). The maximum calculated power factor ($S^2\sigma$) of the Si / PEDOT:PSS interface was 1.24 uW/K^2-cm with a 15.25 nm thick PEDOT:PSS layer. Compared to the power factor of pristine PEDOT:PSS (Table 1, 0.47 uW/K^2-cm), we found a near 10 times increase in the power factor using the Si /

PEDOT:PSS interface. The increase in power factor of our Si / PEDOT:PSS interface was caused by the enhancement of the Seebeck coefficient, which was the focus of this research. When compared against other PEDOT:PSS composite thermoelectric materials, the results of this work showed a higher power factor than the previously mentioned tellurium nanowire composite, as well as a comparable power factor with a bismuth telluride powder composite (Figure 22). However, when comparing against the power factor of modern thermoelectrics (Table 1, 43.32 uW/ K^2-cm), it could be seen that our Si / PEDOT:PSS interface power factor is still about an order of magnitude smaller. But even though the interface we have created could not compete with modern thermoelectric material performance, our results prove that interface effects between materials, such as PEDOT:PSS and silicon, can result in an increased Seebeck coefficient and should be explored further.
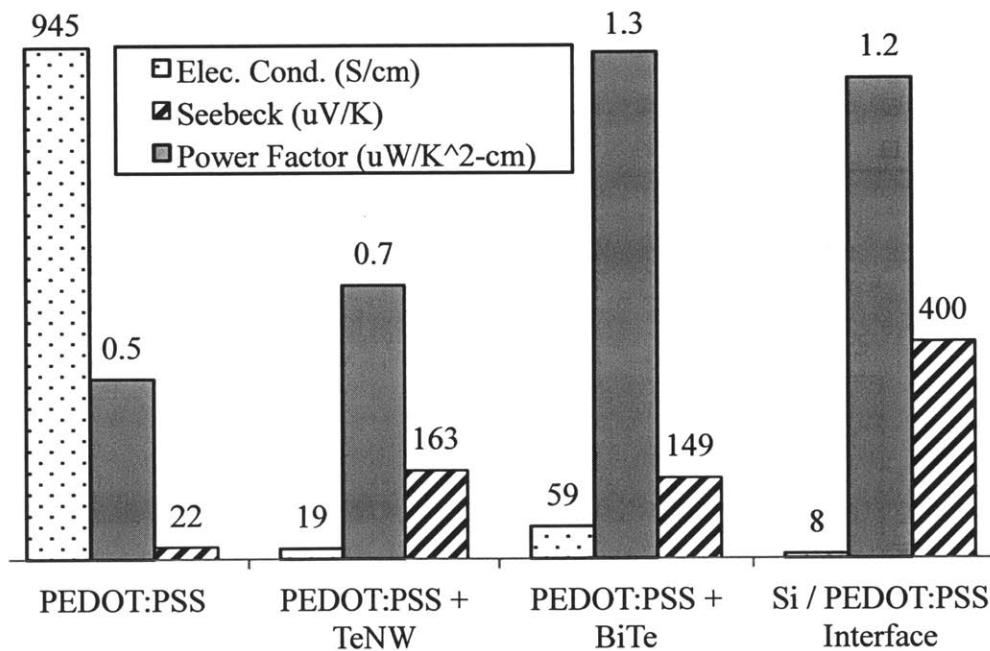

Figure 22: The electrical conductivity (dotted), Seebeck coefficient (striped), and power factor (solid) of PEDOT:PSS,[4] composite materials of PEDOT:PSS with tellurium nanowires[5] and bismuth telluride powder,[4] and the Si / PEDOT:PSS interface (this work).

4.4 Future Work

The results from this work have created several avenues for future research to explore and enhance the thermoelectric properties at the interface between two materials. First, the uniformity of the coating of PEDOT:PSS on the silicon substrate was unclear in this study. Further research can be explored into surface preparation techniques, such as coating with polylysine, to create a more hydrophilic surface with more uniform spin coating results. A more uniform PEDOT:PSS surface could yield better interface interaction between the two materials and further enhance the Seebeck coefficient. In addition, even though HF was used in these experiments to remove the oxide layer of the silicon substrate, the surface could have become reoxidized again during the sample preparation because spin coating was performed in an air atmosphere and the substrate was rinsed with water after etching. For future research, precautions should be taken to limit this possible reoxidation of the silicon surface by performing experiments in an inert argon atmosphere and rinsing with a liquid other than water. Oxidation on the surface of the silicon substrate creates an insulating barrier between the silicon and the PEDOT:PSS, which restricts any interface interaction. Ensuring that the silicon oxidation is completely removed could lead to better interface interaction and a further enhanced Seebeck coefficient than the one reported in this research.

Second, the depth of interaction at the interface between the two materials (space charge region) was still unknown. To better explore the depth of the space charge region and its effect on the thermoelectric properties at the interface, the use of a thinner substrate of silicon should be explored. Investigating the properties that exist at the interface of a 10 nm thick PEDOT:PSS layer with a 10 nm thick silicon substrate and 5 nm thick silicon substrate would reveal useful results to better explain the space charge region.

Third, the ability to create 5 nm thick films of conductive polymer PEDOT:PSS should be further explored for use in nanoscale thermoelectric devices. If an n-type semiconducting polymer can be spin coated to make nanoscale thin films using the methodology described in this research, then nanoscale thermoelectric devices could be devised using these materials as the two legs on a thermoelectric device. Nanoscale thermoelectric devices could be used in various areas, such as the microelectronic and biomedical industries, as a way to cool down microchips or generate power at the nanoscale.

Lastly, our results showing the enhancement of Seebeck coefficient values at the PEDOT:PSS and silicon interface should be explored further by combining PEDOT:PSS with other n-type high-Seebeck semiconductors. Single-crystal silicon has a high thermal conductivity[23] which makes it unattractive for thermoelectric applications. Therefore, investigating the thermoelectric properties at the interface between PEDOT:PSS and n-type high-Seebeck semiconductors with low thermal conductivity should be investigated. Additionally, exploring new types of PEDOT:PSS / Si interfaces, such as creating a composite of n-type silicon nanowires in a PEDOT:PSS matrix, could be a promising avenue to create high ZT thermoelectric composite materials that are not only efficient, but also malleable and cheap.

References

1   Office of Energy Efficiency and Renewable Energy, in *EERE Network News*, http://apps1.eere.energy.gov/news/news_detail.cfm/news_id=15650, (2009).

2   National Academy of Sciences, *Our Energy System*, http://needtoknow.nas.edu/energy/interactive/our-energy-system/, (2012).

3   M. S. Dresselhaus, G. Chen, M. Y. Tang, R. Yang, H. Lee, D. Wang, Z. Ren, J.-P. Fleurial, and P. Gogna, ChemInform **38**, (2007).

4   B. Zhang, J. Sun, H. E. Katz, F. Fang, and R. L. Opila, ACS Applied Materials and Interfaces **2**, 3170 (2010).

5   K. C. See, J. P. Feser, C. E. Chen, A. Majumdar, J. J. Urban, and R. A. Segalman, Nano Letters **10**, 4664 (2010).

6   C. Meng, C. Liu, and S. Fan, Advanced Materials **22**, 535 (2010).

7   H. Goldsmid, in *CRC Handbook of Thermoelectrics* (CRC Press, 1995).

8   D. Rowe, in *Thermoelectrics Handbook* (CRC Press, 2005), p. 1.

9   G. Chen, M. S. Dresselhaus, G. Dresselhaus, J. P. Fleurial, and T. Caillat, International Materials Reviews **48**, 45 (2003).

10   A. J. Minnich, M. S. Dresselhaus, Z. F. Ren, and G. Chen, Energy & Environmental Science **2**, 466 (2009).

11   B. Poudel, Q. Hao, Y. Ma, Y. Lan, A. Minnich, B. Yu, X. Yan, D. Wang, A. Muto, D. Vashaee, X. Chen, J. Liu, M. S. Dresselhaus, G. Chen, and Z. Ren, Science **320**, 634 (2008).

12   Q. Yao, L. Chen, W. Zhang, S. Liufu, and X. Chen, ACS Nano **4**, 2445 (2010).

13   O. P. Dimitriev, D. A. Grinko, Y. V. Noskov, N. A. Ogurtsov, and A. A. Pud, Synthetic Metals **159**, 2237 (2009).

14   A. M. Nardes, R. A. J. Janssen, and M. Kemerink, Advanced Functional Materials **18**, 865 (2008).

15   H. Yan and H. Okuzaki, Synthetic Metals **159**, 2225 (2009).

16   J. R. Ehrstein, M. C. Croarkin, and H. K. Liu, edited by U. S. D. o. C. NIST (2006).

17   N. Cusack and P. Kendall, Proceedings of the Physical Society **72**, 898 (1958).

18   A. T. Burkov, A. Heinrich, P. P. Konstantinov, T. Nakama, and K. Yagasaki, Measurement Science and Technology **12**, 264 (2001).

19   J. Ouyang, Q. Xu, C.-W. Chu, Y. Yang, G. Li, and J. Shinar, Polymer **45**, 8443 (2004).

20   A. M. Nardes, *On the conductivity of PEDOT:PSS thin films* (Technische Universiteit Eindhoven, 2007).

21   G. Vazquez, E. Alvarez, and J. M. Navaza, Journal of Chemical & Engineering Data **40**, 611 (1995).

22   L. He, C. Jiang, H. Wang, D. Lai, and Rusli, Applied Physics Letters **100**, 073503 (2012).

23   S. Uma, A. D. McConnell, M. Asheghi, K. Kurabayashi, and K. E. Goodson, International Journal of Thermophysics **22**, 605 (2001).